Elastic Proton-Deuteron Backward Scattering: Relativistic Effects and Polarization Observables

L.P. Kaptari[a,b], B. Kämpfer[a], S.M. Dorkin[d], S.S. Semikh[b]

[a]Research Center Rossendorf, Institute for Nuclear and Hadron Physics,
PF 510119, 01314 Dresden, Germany

[b]Bogoliubov Laboratory of Theoretical Physics, JINR Dubna,
P.O. Box 79, Moscow, Russia

[d] Far-Eastern State University, Vladivostok, Russia

Abstract

The elastic proton-deuteron backward reaction is analyzed within a covariant approach based on the Bethe-Salpeter equation with realistic meson-exchange interaction. Lorentz boost and other relativistic effects in the cross section and spin correlation observables, like tensor analyzing power and polarization transfer etc., are investigated in explicit form. Results of numerical calculations for a complete set of polarization observables are presented.

key words: elastic proton-deuteron scattering, Bethe-Salpeter equation,
polarization observables

PACS number(s): 21.45+v, 21.10.Ky, 21.60.-n

1 Introduction

Presently a wideranging program of precisely investigating the structure of the lightest nuclei is under consideration. There are new proposals to study the polarization characteristics of the deuteron using both hadronic [1, 2] and electromagnetic probes (cf. [3, 4]). Besides the goal of checking fundamental results of quantum chromodynamics (for instance, the study of the Q^2 evolution of the Gerasimov-Drell-Hearn sum rule [3]) the envisaged experiments focus on a complete reconstruction of the amplitude of the corresponding process [1, 4, 5] and an overall investigation of the nuclear momentum distribution [2, 6].

The simplest reactions with hadron probes are processes of forward or backward scattering of protons off the deuteron. The extensive experimental study of these reactions has started a decade ago in Dubna and Saclay (cf. [6, 7, 8, 9]) and is planned to be continued in the nearest future at COSY [2]. One may classify this type of reactions as inclusive break-up processes, exclusive quasi-elastic scattering and elastic processes. A common feature of these processes is that in a collinear geometry, the measured momenta of the fragments are directly connected with the argument of the deuteron wave function in the momentum space, supposed the reaction mechanism is dominated by the one-nucleon exchange. In such a way a direct experimental investigation of the momentum distribution within the deuteron in a large interval of internal momenta seems to be accessible. By using polarized particles one may investigate as well different aspects of spin-orbit interaction in the deuteron and obtain hints on the role of non-nucleon degrees of freedom in the deuteron wave function, like Δ isobars, $N\bar{N}$ excitations and so on. An encouraging fact here is that the extracted momentum distributions from different reactions with electromagnetic and hadron probes are rather similar, and therefore a realization of experimental programs at different facilities may provide a quite complete information on the internal structure of the deuteron.

Nowadays the elastic proton-deuteron (pD) backward scattering with both polarized protons and deuterons receives a renewed interest [2]. A distinguished peculiarity of this process is that within the impulse approximation the cross section is proportional to the fourth power of the deuteron wave function, contrary to the break-up and quasi-elastic reactions which are proportional to the second power of the wave function. This makes the processes of elastic scattering much more sensitive to the theoretically assumed mechanisms, and even a slight modification of the deuteron wave function may result in significant deviations from the calculated cross section. However, as pointed out by Vasan [10], Frankfurt and Strikman [11] and Karmanov [12] the polarization observables, like

tensor analyzing power and polarization transfer, are exactly as those obtained for the break-up and quasi-elastic scattering in the non-relativistic limit. Beyond both the non-relativistic limit and the impulse approximation the polarization observables differ for different processes. Hence, a combined analysis of data on polarization characteristics from the above mentioned three processes will constrain the basic reaction mechanism and the role of non-nucleon degrees of freedom and relativistic effects in the deuteron. Another peculiarity of elastic backward or forward pD reactions is that the amplitude of the processes is determined by only four complex helicity amplitudes, and a complete reconstruction of these amplitudes seems possible in one experimental set-up. For this it is sufficient to measure 10 independent observables as proposed in refs. [5, 13]. Certainly this does not mean that the realization of such an exhausting experiment will determine entirely the deuteron structure; only within the non-relativistic impulse approximation the cross section is directly related to the deuteron wave function.

First measurements of polarization observables, such as the tensor analyzing power T_{20} and polarization transfer κ, have been performed in Dubna [7, 14, 15] and Saclay [8, 9]. Theoretically the elastic pD scattering has been studied by many authors [16, 17, 18, 19, 20]. It has been shown that the cross section can not be satisfactorily described within the non-relativistic impulse approximation and that other mechanisms, e.g., described by meson-exchange triangle diagrams [19, 20], are important. Besides the importance of other mechanisms, the role of relativistic corrections within the impulse approximation has been studied by several authors already some time ago (see [17, 18] and further references therein) within the Bethe-Salpeter (BS) formalism. The unpolarized cross section and the tensor analyzing power have been numerically computed in a fully covariant way and a comparison with polarization data, available at this time, has been made. However, in view of the present experimental situation and future proposals [1, 2, 5, 13] a detailed covariant investigation of the role of relativistic corrections, such as Lorentz boost effects and contributions of negative-energy waves etc. is still lacking. In the present paper an attempt is presented to fill this gap.

We focus here on a detailed study of the elastic pD amplitude within the BS approach by using the numerical solution obtained with a realistic one-boson exchange interaction [21, 22]. It is known that one of the unpleasant features within the BS formalism is the cumbersomeness of the final expressions for the calculated observables and difficulties in their physical interpretation (cf. refs. [17, 23, 24]). In this paper we try to avoid this problem and present our results in a form as simple as possible. For this sake we separate the contributions of the positive-energy waves and identify them in the non-relativistic

limit. The contributions of the Lorentz boost effects and the negative-energy waves in the deuteron are then calculated in leading order. That means, in the fully covariant results we keep the first orders of negative-energy P waves and the leading-order terms of a Taylor expansion. In this way we are able to separate and to investigate in explicit form the contribution of the Lorentz boost effects and negative-energy waves to the amplitude, cross section and polarization observables as well. Results of numerical calculations for a complete set of observables are also presented.

Our paper is organized as follows: In section II the kinematics of the process is described, and the covariant amplitude is derived in details in section III. Since the covariant expressions within the BS approach are rather lengthy and since in the procedure of the arrangement of results in parts containing non-relativistic formulae and boost effects and relativistic corrections separately, it is very important to provide a clear definition of all the relevant variables. In sections IV - VI a complete set of polarization observables is defined in terms of BS wave functions. The non-relativistic limit, Lorentz boost effects and relativistic corrections are studied analytically and numerically for the cross section and for a class of polarization observables. A comparison with available experimental data is also made. In section VII an interpretation of the relativistic corrections in terms of non-relativistic meson-exchange like contributions is performed. To do so we solve the BS equation for the negative-energy P waves in the one-iteration approximation and express explicitly the ${}^3P_1^{+-}$ and ${}^1P_1^{+-}$ waves via the non-relativistic S and D waves of the deuteron. The obtained result for the elastic amplitude is found in a form being very similar to amplitudes computed in the non-relativistic picture when estimating the role of $N\bar{N}$ pair currents in electromagnetic processes. Some cumbersome expressions and useful formulae are collected in the Appendices A and B.

2 Kinematics

We consider the elastic backward scattering reaction of the type

$$p \,+\, D = p'(\theta = 180^0) \,+\, D'. \tag{1}$$

The differential cross section of the reaction (1) in the center of mass system (c.m.s.) of colliding particles reads

$$\frac{d\sigma}{d\Omega} \,=\, \frac{1}{64\pi^2 s}\,|\mathcal{M}\,|^2, \tag{2}$$

where s is the Mandelstam variable denoting the total energy squared in the c.m.s., and $\mathcal{M}$ is the invariant amplitude of the process. In the case of backward scattering the cross

section eq. (2) depends only on one kinematical variable which usually is chosen as s. Other variables can be expressed via s by using energy conservation. For instance, the Mandelstam variable u is $u = (M_d^2 - m^2)^2/s$, while the c.m.s. momentum is $\boldsymbol{p}^2 = -t/4$ etc. Here M_d and m stand for the deuteron and nucleon masses, respectively. Then in the c.m.s we define the relevant kinematical variables as follows: the four-momenta of particles read

$$D = (E, \boldsymbol{p}),\ p = (\epsilon, -\boldsymbol{p}),\ D' = (E, -\boldsymbol{p}),\ p' = (\epsilon, \boldsymbol{p}), \tag{3}$$

and the polarization four-vectors of the deuteron with polarization indices M and M' can be written as

$$\xi_M = (\frac{\boldsymbol{p}\boldsymbol{\xi}_M}{M_d}, \boldsymbol{\xi}_M + \boldsymbol{p}\frac{\boldsymbol{p}\boldsymbol{\xi}_M}{M_d(E+M_d)}) \tag{4}$$

$$\xi'_{M'} = (-\frac{\boldsymbol{p}\boldsymbol{\xi}'_{M'}}{M_d}, \boldsymbol{\xi}'_{M'} + \boldsymbol{p}\frac{\boldsymbol{p}\boldsymbol{\xi}'_{M'}}{M_d(E+M_d)}), \tag{5}$$

where $\boldsymbol{\xi}, \boldsymbol{\xi}'$ are the three-polarization vectors in the rest frame of the deuteron,

$$\boldsymbol{\xi}_{+1} = (-1, i, 0)/\sqrt{2}, \quad \boldsymbol{\xi}_{-1} = (1, i, 0)/\sqrt{2}, \quad \boldsymbol{\xi}_0 = (0, 0, 1). \tag{6}$$

The proton spinors are normalized as $\bar{u}(p)u(p) = 2m$ with

$$u(\boldsymbol{p}, s) = \sqrt{m+\epsilon}\begin{pmatrix} \chi_s \\ -\frac{\boldsymbol{\sigma}\boldsymbol{p}}{m+\epsilon}\chi_s \end{pmatrix} \qquad u(\boldsymbol{p}', s') = \sqrt{m+\epsilon}\begin{pmatrix} \chi_{s'} \\ \frac{\boldsymbol{\sigma}\boldsymbol{p}}{m+\epsilon}\chi_{s'} \end{pmatrix}, \tag{7}$$

where χ_s denotes the usual two-dimensional Pauli spinor.

In what follows we shall widely exploit as variable the momentum of the outgoing proton, P_{lab}, in the rest frame of the incoming deuteron, which we here define as laboratory system. The relation between c.m.s. and laboratory system is simply expressed by $|\boldsymbol{p}| = 2mP_{lab}/\sqrt{u}$.

Now we proceed with an analysis of the general properties of the invariant amplitude $\mathcal{M}$. In principle, the amplitude $\mathcal{M}$ for the elastic fermion-vector–boson scattering has been studied in detail and is well known (see, for instance refs. [5, 13, 25]), nevertheless for the sake of completeness we present here some of the most important characteristics of $\mathcal{M}$.

The process of the elastic pD scattering is determined by 12 independent partial amplitudes [25]. However, in case of forward or backward scattering, due to the conservation of the total helicity of colliding particles, only four amplitudes remain independent, and these four amplitudes determine all the possible polarization observables of the process.

There are many ways of representing these four amplitudes. In order to emphasize explicitly the transition between initial and final states with fixed helicities it is convenient to represent $\mathcal{M}$ in the c.m.s. in a two-dimensional spin space for the proton spinors and three-dimensional space for the deuteron spin characteristics. In this case the manifest covariance of the amplitude is lost. However the analysis and final formulae become much simpler and transparent. Moreover, by making use of eqs. (3) - (7) all the polarization characteristics of the reaction may be expressed via the corresponding quantities evaluated in the deuteron rest frame. This gives another advantage of such an analysis, namely it allows for a straightforward non-relativistic limit, in particular avoiding the problem of boosting or not the non-relativistic polarization vectors from the rest frame to the c.m.s. It is worth emphasizing that in such a representation of the invariant amplitude, in spite of the fact that it is not explicitly covariant, its form is the most general one and valid in both the relativistic picture and the non-relativistic limit as well.

In this paper we keep our notation as close as possible to the one used in refs. [5, 13]. Hence the total amplitude is written in the form

$$\mathcal{M} = \chi^+_{s'}\, \mathcal{F}\, \chi_s \tag{8}$$

with

$$\mathcal{F} = \mathcal{A}\,(\boldsymbol{\xi}_M \boldsymbol{\xi}^+_{M'}) + \mathcal{B}\,(\boldsymbol{n}\boldsymbol{\xi}_M)(\boldsymbol{n}\boldsymbol{\xi}^+_{M'}) + i\mathcal{C}\,(\boldsymbol{\sigma}\cdot[\boldsymbol{\xi}_M \times \boldsymbol{\xi}^+_{M'}]) + i\mathcal{D}\,(\boldsymbol{\sigma}\boldsymbol{n})(\boldsymbol{n}\cdot[\boldsymbol{\xi}_M \times \boldsymbol{\xi}^+_{M'}]), \tag{9}$$

where $\boldsymbol{n}$ is a unit vector parallel to the beam direction; $\mathcal{A}, \mathcal{B}, \mathcal{C}$ and $\mathcal{D}$ are the partial amplitudes of the pD elastic scattering process depending on the initial energy. Then the cross section (2) is determined by $\mathrm{Tr}(\mathcal{F}^+\,\mathcal{F})$. In the following we suppress the subscripts M and M' of the polarization vectors ξ, bearing in mind that in computing observables the summation over these indices results in the completeness relation for ξ or in the polarization density matrix of the deuteron, which reads in covariant form [26]

$$\sum_M \xi^\mu_M \xi^{+\nu}_M \;=\; \left(-g_{\mu\nu} + \frac{D^\mu D^\nu}{M_d^2}\right), \tag{10}$$

$$\begin{aligned}\rho_{\mu\nu} \;=\; & \frac{1}{3}\left(-g_{\mu\nu} + \frac{D_\mu D_\nu}{M_d^2}\right) + \frac{1}{2M_d} i\epsilon_{\mu\nu\gamma\delta} D^\gamma \mathcal{S}^\delta_D \\ & + \left\{-\frac{1}{2}\left((W_{\lambda_1})_{\mu\rho}(W_{\lambda_2})^\rho{}_\nu + (W_{\lambda_2})_{\mu\rho}(W_{\lambda_1})^\rho{}_\nu\right)\right. \\ & \left. -\frac{2}{3}\left(-g_{\lambda_1\lambda_2} + \frac{D_{\lambda_1} D_{\lambda_2}}{M_d^2}\right)\left(-g_{\mu\nu} + \frac{D_\mu D_\nu}{M_d^2}\right)\right\} Q_D^{\lambda_1\lambda_2},\end{aligned} \tag{11}$$

where $(W_\lambda)_{\mu\nu} \equiv i\epsilon_{\mu\nu\gamma\lambda} D^\gamma / M_d$; $\mathcal{S}_D$ is the spin vector, and Q_D stands for the alignment tensor of the deuteron. $\mu, \nu, \lambda \cdots$ are Lorentz indices, and we use the metric $g_{\mu\nu}$ with signature -2.

In the three-dimensional representation for the deuteron polarization and two-dimensional Pauli matrices for the nucleon states the corresponding density matrices can be cast in the simple form

$$\rho_p = \frac{1}{2}\left(I + (\boldsymbol{\sigma}\,\mathbf{P}_p)\right), \tag{12}$$

$$\rho^{\alpha\beta} = \frac{1}{3}\left(\delta_{\alpha\beta} - \frac{3}{2} i\epsilon^{\alpha\beta\delta}\tilde{\mathcal{S}}_D^{\delta} - 2\,\tilde{Q}_D^{\alpha\beta}\right), \tag{13}$$

where $\mathbf{P}_p$ is the proton polarization three-vector, $\tilde{\mathcal{S}}_D$ and $\tilde{Q}_D$ are spin and tensor polarization operators (actually 3×3 matrices) of the deuteron.

3 The one-nucleon exchange mechanism

We investigate here the relativistic one-nucleon exchange defined by the diagram depicted in fig. 1. Using the kinematics shown in fig. 1 and working with the Mandelstam technique [27], the one-nucleon exchange contribution to the elastic amplitude within the BS formalism is

$$\mathcal{M} = \bar{u}(p')\,\Gamma(D,q)\,\tilde{S}_2\,\bar{\Gamma}(D',q')\,u(p). \tag{14}$$

$\Gamma(D,q)$ denotes the BS vertex function of the deuteron; $\tilde{S}_2 = 1/\left(\hat{D}/2 - \hat{q} + m\right)$ is the nucleon propagator, and $\bar{\Gamma} = \gamma_0\Gamma^+\gamma_0$. We use the abbreviation $\hat{D} = D^\mu\gamma_\mu$ when contacting a four-vector with Dirac matrices. The momenta q and q' are fixed by the conditions $D/2 + q = p'$ and $D'/2 + q' = p$. The vertex function $\Gamma(D,q)$ is the solution of the BS equation for the deuteron bound state. The BS equation and consequently its solution $\Gamma(D,q)$ are sixteen-component objects in the spinor space. To solve the BS equation and to compute observables within the BS formalism one usually represents the vertex function $\Gamma(D,q)$ as a 4×4 matrix and utilizes a decomposition of $\Gamma(D,q)$ over a complete set of matrices in the sixteen-dimensional spinor space. As mentioned in ref. [24], the choice of the representation of the matrices depends on the special attacked problem. Actually in some calculations it is convenient to combine two representations, namely the complete set of Dirac matrices (to perform explicit numerical calculations) and the so-called ρ spin classification of the partial vertices [28] (to have a more transparent physical interpretation of the obtained results; for details consult ref. [24, 29]). In the present paper we use mainly the ρ spin classification, however the numerical calculations have been performed in terms of the solution of the BS equation obtained in the Dirac basis [21, 22, 30]. Notice that the solution of the BS equation has been obtained in the deuteron rest frame, whereas

considering the amplitude (14) it is seen that at least one vertex $\Gamma(D,q)$ is defined in a system where the deuteron is moving. Obviously in this case one may explicitly boost the vertex $\Gamma(D,q)$ from the rest frame to the c.m.s. and analyze the amplitude (14) in terms of a BS solution at rest and Lorentz boost effects separately. Our experience shows that in this way one obtains rather cumbersome expressions and a relatively simple and physically meaningful analysis of results is straitened. Therefore, we represent the BS vertex function in a covariant form with eight invariant scalar functions (see Appendix A). Observing that in the process depicted in fig. 1, in each vertex $\Gamma(D,q)$ one nucleon is on the mass shell, the part contributing to the amplitude (14) may be written in a form exactly coinciding with the one used, for instance, by Gross [23] or Keister and Tjon [17, 31]:

$$\Gamma(D,q) \;=\; [h_1\hat{\xi} + h_2\frac{(q\xi)}{m}] + [h_5\hat{\xi} + h_6\frac{(q\xi)}{m}]\frac{\hat{D}/2 - \hat{q} + m}{m}, \qquad (15)$$

where h_i are invariant scalar functions depending on the invariants q^2 and Dq. Then after summation over the spins in eq. (2) one gets the cross section in a fully covariant form in terms of the relativistic BS solutions $\Gamma(D,q)$ as

$$\frac{d\sigma}{d\Omega} \;=\; \frac{1}{64\pi^2 s}\,\frac{1}{6}\mathrm{Tr}\left[(\hat{p}\,' + m)\Gamma(D,q)\tilde{S}_2\bar{\Gamma}(D',q')(\hat{p}\,+m)\Gamma(D',q')\tilde{S}_2\bar{\Gamma}(D,q)\right], \qquad (16)$$

where, when replacing $\Gamma(D,q)$ by eq. (15) and summing over the deuteron spins, one should make use of eqs. (10) or (11) in dependence of the initial and final states of the particles in a concrete measurement.

Eq. (16) together with eqs. (10) and (11) completely determine all characteristics of the process. When computing the trace in eq. (16) one obtains a fully covariant relativistic expression of all observables. In our calculations we use a suitable algebraic formula manipulation code which, within the representation of the solution of the BS equation in the form (15), delivers the covariant, but rather cumbersome results (for examples cf. ref. [17]). These results have been tested by evaluating the non-relativistic limits for the cross section and polarization observables. However, further investigations relying on these lengthy analytical expressions seem to be almost impossible. Therefore, for an explicit study of the influence of the Lorentz boost effects and other relativistic corrections we shall investigate different aspects of the amplitude $\mathcal{M}$ in eq. (2) instead of the cross section (16).

By substituting eq. (15) into eq. (14) and making use of the Gordon identity, $\bar{u}(p',s')[\hat{a}(\hat{p}-m) + (\hat{p}'-m)\hat{a}]u(p,s) = 0$, one can represent the amplitude in the form

$$\mathcal{M} = \sum_{i=1}^{6} \tilde{R}_i\,\bar{u}(p')\,R_i\,u(p) \qquad (17)$$

with six invariant scalar functions $\tilde{R}_i$ and six covariant spin structures defined as

$$R_1 = \hat{\xi}\hat{\xi}', \quad R_2 = \frac{p\xi'}{m}\frac{p'\xi}{m}, \quad R_3 = \hat{\xi}\frac{p\xi'}{m} + \hat{\xi}'\frac{p\xi'}{m}, \quad R_4 = \hat{\xi}(\hat{D} - \hat{p}')\hat{\xi}', \tag{18}$$

$$R_5 = \frac{p\xi'}{m}\frac{p'\xi}{m}(\hat{D} - \hat{p}'), \quad R_6 = \hat{\xi}(\hat{D} - \hat{p}')\frac{p\xi'}{m} + (\hat{D} - \hat{p}')\hat{\xi}'\frac{p'\xi}{m}, \tag{19}$$

$$\tilde{R}_1 = \frac{1}{m}(2h_1h_5^* + h_5h_5^*) - \frac{mh_1h_1^*}{(D-p')^2 - m^2}, \tag{20}$$

$$\tilde{R}_2 = \frac{1}{m}(h_6h_6^* + 2h_2h_6^*) - \frac{mh_2h_2^*}{(D-p')^2 - m^2}, \tag{21}$$

$$\tilde{R}_3 = \frac{1}{m}(h_1h_6^* + h_2h_5^* + h_5h_6^*) - \frac{mh_1h_2^*}{(D-p')^2 - m^2}, \tag{22}$$

$$\tilde{R}_4 = \frac{h_1h_1^*}{(D-p')^2 - m^2} + \frac{h_5h_5^*}{m^2}, \tag{23}$$

$$\tilde{R}_5 = \frac{h_2h_2^*}{(D-p')^2 - m^2} + \frac{h_6h_6^*}{m^2}, \tag{24}$$

$$\tilde{R}_6 = \frac{h_1h_2^*}{(D-p')^2 - m^2} + \frac{h_5h_6^*}{m^2}. \tag{25}$$

At first glance there seems to be a contradiction between eqs. (18) and (19) and the general expression (9), namely instead of four amplitudes our result contains six different structures. However it is straightforward to prove that the six covariant spin structures in eqs. (18) and (19) in the collinear kinematics reduce to exactly four independent forms. For instance, taking into account that, in case of forward or backward elastic scattering, the expression $(\hat{D} - \hat{p}')$ has no spatial component in the c.m.s. the three structures R_2, R_5 and R_6 are equivalent and determine the amplitude $\mathcal{B}$ in eq. (9) (see below). The structure $\hat{\xi}\,\hat{\xi}'$ may be cast into the form of eq. (9) by exploiting Dirac's matrix algebra,

$$\hat{\xi}\,\hat{\xi}' = (\xi\xi') \; - \; i\xi_\mu\xi'_\nu\,\sigma^{\mu\nu} = (\xi\xi') \; + \gamma_0(\vec{\mathcal{P}}_1\vec{\gamma}) + i\gamma_0\gamma_5(\vec{\mathcal{P}}_2\vec{\gamma}), \tag{26}$$

$$\vec{\mathcal{P}}_1 \equiv (\xi_0\vec{\xi}' + \xi'_0\vec{\xi}), \quad \vec{\mathcal{P}}_2^{\,\rho} \equiv \epsilon_{\alpha\beta\rho}\xi_\alpha\xi'_\beta; \quad \alpha, \beta, \rho = 1, 2, 3. \tag{27}$$

Then it is seen that among the six amplitudes eqs. (18) and (19) only four are independent in collinear kinematics. The correspondence between eq. (9) and eqs. (18) and (19) becomes obvious if the former are written in the c.m.s. In this case,

$$\begin{aligned} \bar{u}(p', s')\, R_1\, u(p, s) \;\; &= \;\; \chi^+_{s'}\Big[-(\boldsymbol{\xi}\boldsymbol{\xi}')2\epsilon - i\boldsymbol{\sigma}(\boldsymbol{\xi}\times\boldsymbol{\xi}')\frac{E}{M_d}2m \\ &+ \;\; i(\boldsymbol{\sigma}\boldsymbol{p})(\boldsymbol{p}, \boldsymbol{\xi}\times\boldsymbol{\xi}')\frac{(m+\epsilon)^2 - (M_d+E)^2}{M_d(M_d+E)(m+\epsilon)} + \frac{\boldsymbol{p}\boldsymbol{\xi}}{M_d}\frac{\boldsymbol{p}\boldsymbol{\xi}'}{M_d}(4E - 4\epsilon)\Big]\,\chi_s, \end{aligned} \tag{28}$$

$$\bar{u}(p',s')\,R_2\,u(p,s) = -\frac{2\epsilon(E-\epsilon)^2}{m^2}\chi^+_{s'}\left[\frac{\boldsymbol{p\xi}}{M_d}\frac{\boldsymbol{p\xi}'}{M_d}\right]\chi_s, \tag{29}$$

$$\begin{aligned}\bar{u}(p',s')\,R_3\,u(p,s) &= \frac{E-\epsilon}{M_d m} \\ &\times\ \chi^+_{s'}\left[4mM_d\frac{\boldsymbol{p\xi}}{M_d}\frac{\boldsymbol{p\xi}'}{M_d}+2i\boldsymbol{\sigma}(\boldsymbol{\xi}\times\boldsymbol{\xi}')p^2-2i(\boldsymbol{\sigma p})(\boldsymbol{p},\boldsymbol{\xi}\times\boldsymbol{\xi}')\right]\chi_s,\end{aligned} \tag{30}$$

$$\begin{aligned}\bar{u}(p',s')\,R_4\,u(p,s) &= -(E-\epsilon)\chi^+_{s'}\Bigg[\qquad\qquad -(\boldsymbol{\xi\xi}')2m+i(\boldsymbol{\sigma p})(\boldsymbol{p},\boldsymbol{\xi}\times\boldsymbol{\xi}') \\ &\times\ \frac{(M_d+E-m-\epsilon)^2}{M_d(M_d+E)(m+\epsilon)}+i\boldsymbol{\sigma}(\boldsymbol{\xi}\times\boldsymbol{\xi}')\frac{2(\epsilon^2-m^2-E\epsilon)}{M_d}\Bigg]\chi_s,\end{aligned} \tag{31}$$

$$\bar{u}(p',s')\,R_5\,u(p,s) = -\frac{2(E-\epsilon)^3}{m}\chi^+_{s'}\left[\frac{\boldsymbol{p\xi}}{M_d}\frac{\boldsymbol{p\xi}'}{M_d}\right]\chi_s, \tag{32}$$

$$\bar{u}(p',s')\,R_6\,u(p,s) = -\frac{4(E-\epsilon)^3}{m}\chi^+_{s'}\left[\frac{\boldsymbol{p\xi}}{M_d}\frac{\boldsymbol{p\xi}'}{M_d}\right]\chi_s. \tag{33}$$

It is worth stressing again that, in spite of these six covariant spin structures $R_1\cdots R_6$ being written in c.m.s. have lost their explicit covariance, they still determine the covariant amplitude $\mathcal{M}$ of the process. The corresponding invariant scalar functions $\tilde{R}_i$ defined by eqs. (20) - (25) may be computed in any reference frame. Since the numerical solutions [22] of the BS equation have been obtained in the deuteron rest frame, we also express $\tilde{R}_i$ in this system. When one nucleon is on the mass shell, i.e. $M_d/2+q_0=E'_p$, the invariant functions h_i are of the form (see Appendix A)

$$\sqrt{4\pi}h_1 = \frac{1}{\sqrt{2}}g_1-\frac{1}{2}g_3+\frac{\sqrt{3}m}{2M_dP_{lab}}(2E'_p-M_d)g_5, \tag{34}$$

$$\sqrt{4\pi}h_2 = -\frac{m}{\sqrt{2}(m+E'_p)}g_1-\frac{m(m+2E'_p)}{2P^2_{lab}}g_3+\frac{\sqrt{3}m}{2P_{lab}M_d}(2M_d-E'_p)g_5, \tag{35}$$

$$\sqrt{4\pi}h_5 = -\frac{\sqrt{3}mE'_p}{2M_dP_{lab}}g_5, \tag{36}$$

$$\sqrt{4\pi}h_6 = -\frac{m^2}{\sqrt{2}M_d(m+E'_p)}g_1+\frac{(E'_p+2m)m^2}{2M_dP^2_{lab}}g_3+\frac{\sqrt{6}m^2}{2M_dP_{lab}}g_7, \tag{37}$$

where g_i are the BS vertex functions in the deuteron rest system and all the kinematical variables in eqs. (34) - (37) should be evaluated in this system.

4 Observables

Having determined the amplitude by eqs. (17) - (37) one may define various polarization characteristics of the process. Employing the notation used in refs. [5, 13, 25] we define

the set of all possible polarization observables for the non-covariant amplitude (8) by

$$\mathcal{H}_{\lambda,H\to\lambda',H'} = \frac{\mathrm{Tr}\left(\mathcal{F}\sigma_\lambda \mathcal{D}_H \mathcal{F}^+ \sigma_{\lambda'} \mathcal{D}_{H'}\right)}{\mathrm{Tr}\left(\mathcal{F}\mathcal{F}^+\right)}, \tag{38}$$

where the subscripts λ and H (λ' and H') refer to the polarization characteristics of the initial (final) proton and deuteron respectively; σ_λ is the Pauli matrix, and $\mathcal{D}$ stands for a set of 3×3 operators defining the deuteron polarization. Note that the introduced subscripts may appear as either single index or double indices in dependence on the reaction conditions. For instance, $0,0 \to 0,0$ means a process with unpolarized particles, while $0, NN \to 0, NN$ means the tensor-tensor polarization of the initial and final deuterons parallel to the normal of the reaction plane direction.

At this point it is worth mentioning that the numerical solution of the BS equation has been obtained in the Euclidean space-time with imaginary time component q_0 of the relative momentum q. In the process under consideration q_0 is fixed and real. Hence, one needs either a numerical procedure for an analytical continuation of the amplitudes to the real relative energy axis (cf. [17]) or another recipe [32] for using the numerical solutions in this case.

We rely on the analysis of the BS partial vertices performed in ref. [24], where the dependence of S and D wave vertices upon the relative energy is shown to be smooth, contrary to the amplitudes which display a strong dependence on q_0. Therefore, in our calculations, we can replace, at moderate values of q_0, the S and D vertices by their values at $q_0 = 0$ with good accuracy. The P vertices can be expanded into Taylor series around $q_0 = 0$ up to a desired order in p_0/m. Then the corresponding derivatives can be computed numerically along the imaginary axis since they are analytical functions of q_0 [32].

Finally, to cast our formulae in a more familiar form, known from non-relativistic calculations, we introduce the notion of BS wave functions [17, 23, 24]

$$\Psi_S(|\mathbf{P}_{lab}|) = \mathcal{N}\frac{g_1(0,|\mathbf{P}_{lab}|)}{2E'_p - M_D}, \quad \Psi_D(|\mathbf{P}_{lab}|) = \mathcal{N}\frac{g_3(0,|\mathbf{P}_{lab}|)}{2E_2 - M_D}, \tag{39}$$

$$\Psi_{P_5}(|\mathbf{P}_{lab}|) = \mathcal{N}\frac{g_5(0,|\mathbf{P}_{lab}|)}{M_D}, \quad \Psi_{P_7}(|\mathbf{P}_{lab}|) = \mathcal{N}\frac{g_7(0,|\mathbf{P}_{lab}|)}{M_D}, \tag{40}$$

where $\mathcal{N} = 1/4\pi\sqrt{2M_D}$. Then the cross section (16) and the amplitude (9) may be computed in terms of positive and negative-energy wave functions, $\Psi_{S,D}$ and Ψ_{P_5,P_7} respectively. The BS wave functions $\Psi_{S,D}$ are intimately related to the famous non-relativistic deuteron wave functions $u(P_{lab}), w(P_{lab})$, and at small values of P_{lab} they practically coincide [24]. Therefore, their contribution to the amplitudes and cross section is henceforth

referred to as the non-relativistic result. The parts containing the negative-energy waves Ψ_{P_5,P_7} are of a purely relativistic origin and consequently they manifest genuine relativistic correction effects. The weights of these wave functions are quite small [24, 33] and we shall neglect all the terms proportional to $\Psi^2_{P_5,P_7}$; only interferences between $\Psi_{S,D}$ and Ψ_{P_5,P_7} are kept in our results. Besides the mentioned relativistic effects there is another source of relativistic corrections, namely the so-called Lorentz boost effects stemming from the transformation of the BS wave functions from the c.m.s. to the deuteron rest frame.

5 Lorentz boost effects

A straightforward way to study effects of the Lorentz boost is to compare the non-relativistic results with those obtained in the BS formalism by equating to zero all contributions from the negative-energy waves leaving only the contribution of the waves $\Psi_{S,D}$. In the non-relativistic case, the cross section and the spin amplitudes take a simple form [5, 13]

$$\frac{d\sigma_{NR}}{d\Omega} = 3\left(u^2(q)+w^2(q)\right)^2, \tag{41}$$

$$\mathcal{A}_{NR} = \left(u(q)+\frac{w(q)}{\sqrt{2}}\right)^2, \tag{42}$$

$$\mathcal{B}_{NR} = -\frac{3}{2}w(q)\left(2\sqrt{2}u(q)-w(q)\right), \tag{43}$$

$$\mathcal{C}_{NR} = \left(u(q)+\frac{w(q)}{\sqrt{2}}\right)\left(u(q)-\sqrt{2}w(q)\right), \tag{44}$$

$$\mathcal{D}_{NR} = \frac{3}{\sqrt{2}}w(q)\left(u(q)+\frac{w(q)}{\sqrt{2}}\right), \tag{45}$$

where in eqs. (42) - (45) the relative momentum q and appropriate sign conventions are introduced in the definition of the non-relativistic wave functions $u(q)$ and $w(q)$. Note that in non-relativistic calculations there are ambiguities in treating the internal momentum q. It is not clear in what frame of reference the argument of the non-relativistic wave functions $u(q)$ and $w(q)$ should be evaluated: is q to be computed in the three-body center of mass frame as proposed in ref. [34] or should one use the deuteron rest frame [20] in defining the deuteron wave function? At small momenta these alternatives become identical, however a difference occurs already at intermediate energies $P_{lab} \sim 0.2 \cdots 0.3$ GeV/c. In the covariant BS approach this problem is solved by using invariant amplitudes $h_i(q^2, Dq)$ and by taking into account the boost effects.

Substituting eqs. (28) - (37) into eqs. (16) and (38) and expanding the result into

Taylor series around $P_{lab}^2/2m^2$ and keeping the leading terms we obtain the contribution of positive-energy BS waves in the form

$$\frac{d\sigma_0}{d\Omega} = \frac{12m^2}{s}\left(\Psi_S^2(P_{lab})+\Psi_D^2(P_{lab})\right)^2 P_{lab}^4\left(1+\frac{P_{lab}^2}{2m^2}+\frac{29P_{lab}^4}{16m^4}+\frac{83P_{lab}^6}{32m^6}+\cdots\right), \quad (46)$$

$$\mathcal{A}_0 = 16\pi m P_{lab}^2\left(\Psi_S(P_{lab})-\frac{\Psi_D(P_{lab})}{\sqrt{2}}\right)^2 \mathcal{L}(P_{lab}), \quad (47)$$

$$\mathcal{B}_0 = 16\pi m P_{lab}^2\,\frac{3}{2}\Psi_D(P_{lab})\left(2\sqrt{2}\Psi_S(P_{lab})+\Psi_D(P_{lab})\right)\mathcal{L}(P_{lab}), \quad (48)$$

$$\mathcal{C}_0 = 16\pi m P_{lab}^2\left(\Psi_S(P_{lab})-\frac{\Psi_D(P_{lab})}{\sqrt{2}}\right)\left(\Psi_S(P_{lab})+\sqrt{2}\Psi_D(P_{lab})\right)\mathcal{L}(P_{lab}), \quad (49)$$

$$\mathcal{D}_0 = -16\pi m P_{lab}^2\,\frac{3}{\sqrt{2}}\Psi_D(P_{lab})\left(\Psi_S(P_{lab})-\frac{\Psi_D(P_{lab})}{\sqrt{2}}\right)\mathcal{L}(P_{lab}), \quad (50)$$

where the Lorentz boost effects are represented by $\mathcal{L}(P_{lab})$ defined as

$$\mathcal{L}(P_{lab}) = \left(1+\frac{P_{lab}^2}{4m^2}+\frac{7P_{lab}^4}{8m^4}+\cdots\right). \quad (51)$$

It is seen that the results within the BS approach recover the non-relativistic formulae in the leading order in $P_{lab}^2/2m^2$ and receive additional corrections from the Lorentz boost effects. At small values of P_{lab} these corrections are negligible but at moderate values of P_{lab} they become important and may give up to 30 - 40% contributions in the non-relativistic cross section. Note that within the one-nucleon exchange mechanism, P_{lab} is kinematically restricted so that the Taylor expansion in eqs. (46) - (51) is justified since $P_{lab}^2/2m^2 < 1$ in the whole range of the initial energy $\sqrt{s}$.

The elastic cross section for a process with unpolarized particles evaluated within the BS formalism is shown in fig. 2. The dashed line is the contribution of only positive-energy BS functions Ψ_S and Ψ_D (to be compared with the dotted line which represents the computation of the cross section in the non-relativistic limit with Bonn potential [35]). The long-dashed curve represents the corrections from pure Lorentz boost effects. The solid line is the result of full BS calculations by exploiting the numerical solutions [21, 22, 24] of the BS equation with a realistic kernel with $\pi, \omega, \rho, \sigma, \eta, \delta$ exchanges. Experimental data are taken from refs. [20, 36]. The relativistic effects coming from the negative-energy waves are much smaller and they are not displayed here. From fig. 2 it becomes clear that the Lorentz boost effects become essential at $P_{lab} > 0.5$ GeV/c. This is an understandable effects, since it is expected that the boost corrections should increase with increasing initial energy. Remind that the region $P_{lab} > 0.5$ GeV/c corresponds already to rather high initial energies, say $T_{kin} \sim 6$ GeV. (The kinematics of the process is so that at $\sqrt{s} \to \infty$ the momentum of the detected slow proton becomes $P_{lab} \to 0.75\,m$.)

A comparison with experimental data shows that the one-nucleon exchange mechanism alone does not describe satisfactorily the cross section and that other mechanism should be considered [19, 20]. One should keep in mind, however, that measurements of the cross section in the strict backward direction are rather difficult and many experimental data are presented as extrapolations of $d\sigma/d\Omega$ obtained in nearly backward direction to the exact backward angle [16, 36]. In view of the very strong angular dependence of the cross section the data from different groups differ noticeably (see fig. 2 in ref. [17] and fig. 27 in ref. [16]). This, together with the above mentioned sensitivity of the results to the chosen deuteron wave function, generates uncertainties in a detailed comparisons with data. It is not our aim here to improve the agreement with the data, but we intend to proceed with our methodological study within the well defined framework of the impulse approximation.

The Lorentz boost does not affect at all the polarization characteristics defined by eq. (38), as it should be. For instance, a direct calculation of the cross section eq. (16) with the density matrix (11) results in the known non-relativistic formulae for the tensor analyzing power $T_{20} = -\mathcal{H}_{0,NN\to 0,0}/\sqrt{2}$ and the polarization transfer $\kappa = 3\mathcal{H}_{0,L\to L,0}/2$

$$T_{20}^{NR} = \frac{1}{\sqrt{2}} \frac{-\Psi_D^2(P_{lab}) - 2\sqrt{2}\Psi_S(P_{lab})\Psi_D(P_{lab})}{\Psi_S^2(P_{lab}) + \Psi_D^2(P_{lab})}, \tag{52}$$

$$\kappa^{NR} = \frac{1}{\sqrt{2}} \frac{\Psi_S^2(P_{lab}) - \Psi_D^2(P_{lab}) + \Psi_S(P_{lab})\Psi_D(P_{lab})/\sqrt{2}}{\Psi_S^2(P_{lab}) + \Psi_D^2(P_{lab})}. \tag{53}$$

Observe that in the non-relativistic limit the polarization characteristics eqs. (52) and (53) in the elastic pD elastic scattering exactly coincide with ones in the reactions of inclusive [5, 6] or exclusive [2] deuteron break-up processes. In the relativistic case such simple relations among polarization observables do not hold. From this one may conclude that a combined analysis of data obtained within different processes would allow for an estimate of the role of relativistic corrections in the deuteron wave function.

6 Relativistic corrections

In this section we present results of numerical calculations of the contribution to the polarization observables coming from the negative-energy P waves. We are going to investigate the tensor analyzing power and polarization transfer.

There are two factors of smallness in computing relativistic corrections: the term $P_{lab}^2/2m^2$ and terms proportional to the negative-energy P waves in the BS amplitude. In estimating corrections to eq. (46) we expand the result of the trace operation in eq. (16)

and our results of calculating eqs. (28) - (33) into Taylor series around $P_{lab}^2/2m^2$ and keep only the leading terms relative to negative-energy waves and to $P_{lab}^2/2m^2$. The final results for the relativistic effects reads for the cross section

$$\begin{aligned}
\frac{d\sigma}{d\Omega} &= \frac{d\sigma_0}{d\Omega} + \delta\sigma, \qquad (54)\\
\delta\sigma &= \frac{24\sqrt{6}m^3P_{lab}^3}{\sqrt{s}}(\Psi_S^2+\Psi_D^2)\left(\Psi_S+\sqrt{2}\Psi_D\right)\left(\Psi_{P_5}+\frac{2\sqrt{2}P_{lab}^2}{3m^2}\Psi_{P_7}\right)\\
&\quad+\frac{2\sqrt{6}mP_{lab}^5}{\sqrt{s}}(\Psi_S^2+\Psi_D^2)\left(9\sqrt{2}\Psi_D+33\Psi_S\right)\Psi_{P_5}+\cdots
\end{aligned}$$

and for the tensor analyzing power T_{20}

$$\begin{aligned}
T_{20} &= T_{20}^{NR}+\delta T_{20}, \qquad (55)\\
\delta T_{20} &= -\frac{2\sqrt{3}\left(\Psi_S+\sqrt{2}\Psi_D\right)\left(\Psi_S-\Psi_D/\sqrt{2}\right)^2}{(\Psi_S^2+\Psi_D^2)^2}\frac{m}{P_{lab}}\left(\Psi_{P_5}+\frac{2\sqrt{2}P_{lab}^2}{3m^2}\Psi_{P_7}+\cdots\right)
\end{aligned}$$

and for the polarization transfer κ

$$\begin{aligned}
\kappa &= \kappa^{NR}+\delta\kappa, \qquad (56)\\
\delta\kappa &= \frac{\sqrt{6}\left(\Psi_S-\Psi_D/\sqrt{2}\right)\left[\left(2\sqrt{2}\Psi_D-\Psi_S\right)^2-9\Psi_D^2\right]}{(\Psi_S^2+\Psi_D^2)^2}\frac{m}{P_{lab}}\left(\Psi_{P_5}+\frac{2\sqrt{2}P_{lab}^2}{3m^2}\Psi_{P_7}+\cdots\right).
\end{aligned}$$

It should be stressed that a comparison of the relativistic corrections (55) and (56) with those obtained for the deuteron break-up reaction [29, 37] demonstrates that in the elastic proton-deuteron scattering the polarization observables coincide with the ones in the deuteron quasi-elastic and break-up processes only in the non-relativistic limit. Therefore, the data from these processes all together (cf. [14]) can determine the magnitude of the relativistic corrections and further constrain the deviation of the mechanism of these processes from the simple one-nucleon exchange picture.

In fig. 3 results of calculations of the tensor analyzing power T_{20} in the elastic pD backward reaction are presented. The long-dashed curve is the contribution of only positive-energy BS waves eq. (52), the dotted line represents the pure relativistic corrections in eq. (55), while the solid line is the total result within the BS formalism. Experimental data (open and full circles) are from refs. [7, 14, 15]. For the sake of completeness we present some experimental data for the deuteron break-up processes [6] (triangles) and results of computation of T_{20} within the minimal relativization scheme [38, 39] with the Paris deuteron wave function [40]. In fig. 3 it is seen that the theoretical calculations predict a change of sign in the T_{20} whereas the experimental data from both deuteron

break-up and elastic scattering processes shows that T_{20} remains negative in the whole interval of measured values of P_{lab}. However, calculations with the positive-energy BS wave functions (long-dashed line) together with the relativistic corrections (dotted line) result in a better description of data.

In fig. 4 similar calculations are presented for the polarization transfer κ. The dashed line is the contribution of the positive-energy BS wave functions eq. (53), while relativistic corrections eq. (56) are presented by the dotted line; the solid line is the total BS result. As in the previous results the relativistic corrections in κ are small for small and moderate values of P_{lab}, but become essential at higher values of the initial energies.

7 Other spin observables

As mentioned in ref. [5], one of the goals of the future experiments is a direct reconstruction of the four complex amplitudes (9). For this one needs to measure 7 independent observables, however as seen from the above formulae, all polarization observables are bilinear combinations of the amplitudes (9) so that the necessary number of measurements at given energy increases. A full set of polarisation observables for complete measurement has been proposed in refs. [5, 13]. It is found that 10 spin observables, i.e. the two of the first order, like cross section and tensor analyzing power $\mathcal{H}_{0,NN\to 0,0}$, and 8 spin correlations of the second order, for instance $\mathcal{H}_{0,NN\to 0,NN}$, $\mathcal{H}_{0,NN\to 0,SS}$, $\mathcal{H}_{0,N\to 0,LS}$, $\mathcal{H}_{0,N\to N,0}$, $\mathcal{H}_{N,N\to 0,0}$, $\mathcal{H}_{0,LS\to N,0}$, $\mathcal{H}_{0,LS\to 0,0}$ and $\mathcal{H}_{0,LN\to 0,LN}$ could provide a complete analysis of the spin amplitudes (9).

In the previous section the results of relativistic calculations of the tensor analyzing power and polarization transfer from the initial deuteron to the final proton have been presented. In this section additional calculations of spin-correlation observables of the second order are performed. We consider here the proton vector-vector transfer, the deuteron vector-vector and tensor-tensor transfer coefficients. They read explicitly

$$\mathcal{H}_{N,0\to N,0} \equiv \frac{2\left(3\mathcal{A}^2+2\mathcal{A}\mathcal{B}+\mathcal{B}^2-2\mathcal{C}^2-4\mathcal{C}\mathcal{D}-2\mathcal{D}^2\right)}{\mathrm{Tr}\left(\mathcal{F}\mathcal{F}^+\right)} = \frac{1}{9}\frac{\left(\Psi_S+\sqrt{2}\Psi_D\right)^4}{\left(\Psi_S^2+\Psi_D^2\right)^2} + \quad (57)$$

$$\frac{4\sqrt{6}}{9}\frac{\left(\Psi_S-\Psi_D/\sqrt{2}\right)^2\left(\Psi_S+\sqrt{2}\Psi_D\right)^3}{\left(\psi_S^2+\Psi_D^2\right)^3}\frac{m}{P_{lab}}\left(\Psi_{P_5}+\frac{2\sqrt{2}P_{lab}^2}{3m^2}\Psi_{P_7}+\cdots\right),$$

$$\mathcal{H}_{0,N\to 0,N} \equiv \frac{4\left(\mathcal{A}^2+\mathcal{A}\mathcal{B}+\mathcal{C}^2\right)}{\mathrm{Tr}\left(\mathcal{F}\mathcal{F}^+\right)} = \frac{4}{9}\frac{\left(\Psi_S-\Psi_D/\sqrt{2}\right)^2\left(\Psi_S+\sqrt{2}\Psi_D\right)^2}{\left(\Psi_S^2+\Psi_D^2\right)^2} + \quad (58)$$

$$\frac{4\sqrt{6}}{9}\frac{\left(\Psi_S-\Psi_D/\sqrt{2}\right)^2\left(\Psi_S+\sqrt{2}\Psi_D\right)\left(\Psi_S-2\sqrt{2}\Psi_D)^2-9\Psi_D^2\right)}{\left(\psi_S^2+\Psi_D^2\right)^3}\frac{m}{P_{lab}}\left(\Psi_{P_5}+\frac{2\sqrt{2}P_{lab}^2}{3m^2}\Psi_{P_7}+\cdots\right),$$

$$\mathcal{H}_{0,NN\to 0,SS} \equiv \frac{2\left(-3\mathcal{A}^2+2\mathcal{A}\mathcal{B}+3\mathcal{C}^2+10\mathcal{C}\mathcal{D}+5\mathcal{D}^2\right)}{\mathrm{Tr}\left(\mathcal{F}\mathcal{F}^+\right)}=\frac{1}{4}\frac{\left(2\sqrt{2}\Psi_S+\Psi_D\right)^2\Psi_d^2}{\left(\Psi_S^2+\Psi_D^2\right)^2}+ \quad (59)$$

$$\frac{\sqrt{6}\Psi_D\left(\Psi_S+\sqrt{2}\Psi_D\right)\left(\Psi_S-\Psi_D/\sqrt{2}\right)^2\left(2\sqrt{2}\Psi_S+\Psi_D\right)}{\left(\Psi_S^2+\Psi_D^2\right)^3}\frac{m}{P_{lab}}\left(\Psi_{P_5}+\frac{2\sqrt{2}P_{lab}^2}{3m^2}\Psi_{P_7}+\cdots\right),$$

where the first lines in each of eqs. (57) - (59) display the non-relativistic limit, while the second lines are the corresponding parts of purely relativistic corrections.

Figs. 5 - 7 show these spin-correlation observables according to eqs. (57) - (59) calculated within the BS formalism; they are depicted as solid lines. The dashed lines show the contribution of the positive-energy BS waves (i.e., the non-relativistic limit), while the dotted lines are the relativistic corrections due to the contribution of P waves in the deuteron. It is seen that the relativistic effects for the proton-proton transfer coefficients are negligible (see fig. 5) while for the deuteron-deuteron correlations these effects are essential at $P_{lab} \geq 0.5$ GeV/c.

It is interesting to notice that there are observables which in the non-relativistic limit are exactly zero and therefore consist of relativistic corrections only. For instance the tensor-tensor transfer coefficient $\mathcal{H}_{0,LN\to 0,LN}$ is predicted to vanish in the non-relativistic case, while within the BS formalism one gets

$$\begin{aligned}\mathrm{Tr}\left(\mathcal{F}\mathcal{F}^+\right)\mathcal{H}_{0,LN\to 0,LN} &= 9\left(\mathcal{A}^2+Re\mathcal{A}\mathcal{B}-\mathcal{C}^2\right) \quad (60)\\ &\simeq 54m^4P_{lab}^2\left[\sqrt{2}\Psi_S\left(\Psi_{P_5}+2\sqrt{2}\Psi_{P_7}\right)-\psi_D\left(7\Psi_{P_5}+2\sqrt{2}\Psi_{P_7}\right)\right]^2,\end{aligned}$$

where all the contributions from higher orders in P_{lab}^2/m^2 have been neglected. In spite of the small value of this tensor-tensor correlation (see fig. 8) the measurements of such observables may directly quantify the importance of relativistic P waves in the deuteron.

As a conclusion of this section we emphasize that for some of the computed spin observables the relativistic effects are not too important, whereas for a specific class of observables (like the tensor-tensor correlations) admixtures of P waves in the deuteron may result in important corrections, for instance the coefficient (60) differs from zero only due to relativistic effects in the deuteron.

8 One-iteration approximation

The relativistic corrections in eqs. (55) - (60) are governed by negative-energy P wave states in the deuteron. This can be considered as a hint that admixtures of P waves within the BS approach are related to relativistic corrections by taking into account meson-exchange currents and $N\bar{N}$ pair production diagrams [41] in the non-relativistic picture. To establish a correspondence between our results and the mentioned non-relativistic calculations we estimate the contribution of the relativistic corrections by computing the P wave vertices in the so-called "one-iteration approximation" [42]. The gist of this approximation is as follows: In solving the BS equation by an iteration procedure one puts as zeroth iteration the exact solution of the Schrödinger equation for S and D vertices and zero for other waves; then the P vertices are found by one iteration of the BS equation. Our experience in solving numerically the BS equation shows that it converges rapidly for relatively small momenta < 1 GeV/c. That means when utilizing the exact non-relativistic solutions, after one iteration the resulting P waves are not too far from the full solution.

To obtain analytical expressions for the negative-energy waves we proceed with the mixed BS equation in the sense that the BS vertices are expressed via the BS amplitudes as

$$G(k) = i \int \frac{d^4p}{(2\pi)^4} \frac{\lambda^2_{mes}}{(p-k)^2 - \mu^2} \gamma_{mes}\, \Phi(p)\, \gamma_{mes}, \tag{61}$$

where $G(k)$ and $\Phi(p)$ are the BS vertex and amplitude respectively, λ^2_{mes} denotes the meson-nucleon coupling constant and γ_{mes} the meson-nucleon coupling vertex (for scalar, pseudo-scalar or vector couplings).

Then using the decomposition of $G(k)$ and $\Phi(p)$ in the complete set of spin angular matrices Γ_α (for details consult ref. [24]) the BS equation for partial vertices g_α and amplitudes Φ_α (here α accounts for the ρ spin indices of the corresponding partial amplitude) may be written in the form

$$g_\alpha(k_0, |\vec{k}|) = i \int \frac{d^4p}{(2\pi)^4} d\Omega_k \frac{\lambda^2_{mes}}{(p-k)^2 - \mu^2} \mathrm{Tr}\left[\Gamma^+_\alpha(k_0, -\vec{k}) \gamma_{mes} \Gamma_\beta(p_0, \vec{p}) \gamma_{mes}\right] \Phi_\beta(p_0, |\vec{p}|). \tag{62}$$

Using the standard decomposition of the meson propagator over generalized Legendre functions $Q_l(z)$, where $z = (|\vec{p}|^2 + |\vec{k}|^2 + \mu^2 - (p_0 - k_0)^2)/|\vec{p}||\vec{k}|$, one gets

$$g_\alpha(k_0, |\vec{k}|) = -\lambda^2_{mes} \int \frac{p^2 dp\, dp_0}{4\pi^2} W_{\alpha\beta}(|\vec{k}|, |\vec{p}|)\, \Phi_\beta(p_0, |\vec{p}|), \tag{63}$$

$$W_{\alpha\beta}(k,p) \equiv \sum_{lm} \frac{Q_l(z)}{2\pi|\vec{p}||\vec{k}|} \int d\Omega_k d\Omega_p Y_{lm}(p) Y^*_{lm}(k) \mathrm{Tr}\left[\Gamma^+_\alpha(k_0, -\vec{k}) \gamma_{mes} \Gamma_\beta(p_0, \vec{p}) \gamma_{mes}\right].$$

These expressions are still the exact BS equation in the ladder approximation. Further we assume:

(i) in the first approximation the negative-energy waves are exactly zero, i.e., in eqs. (63) remain only $\Phi_\beta = S^{++}$ and D^{++},

(ii) in the interaction kernel $W_{\alpha\beta}$ and in the vertex functions $g^{++}(p)$ we neglect the dependence on the relative energy, i.e., $W_{\alpha\beta}(k,p) \simeq W_{\alpha\beta}(|\vec{k}|,|\vec{p}|)$ and $g^{++}(p) \simeq g^{++}(0,\vec{p})$,

(iii) the negative-energy waves are obtained by only one iteration of eq. (63).

For the pseudo-scalar isovector exchange we get

$$W_{P_1^{+-}\to S^{++}} = W_{P_1^{-+}\to S^{++}} = \mathcal{N}\left[Q_0(z)|\vec{k}| - Q_1(z)|\vec{p}|\right], \tag{64}$$

$$W_{P_1^{+-}\to D^{++}} = W_{P_1^{-+}\to D^{++}} = \mathcal{N}\sqrt{2}\left[Q_2(z)|\vec{k}| - Q_1(z)|\vec{p}|\right], \tag{65}$$

$$W_{P_3^{+-}\to S^{++}} = -W_{P_3^{-+}\to S^{++}} = \mathcal{N}\sqrt{2}\left[-Q_0(z)|\vec{k}| + Q_1(z)|\vec{p}|\right], \tag{66}$$

$$W_{P_3^{+-}\to D^{++}} = -W_{P_3^{-+}\to D^{++}} = \mathcal{N}\left[-Q_1(z)|\vec{p}| + Q_2(z)|\vec{k}|\right], \tag{67}$$

where $\mathcal{N} = -\sqrt{3}/(2|\vec{p}||\vec{k}|E_k)$, $E_k = \sqrt{k^2+m^2} \sim m$.

We perform further calculations in the coordinate space:

$$\int \frac{p^2 dp}{2|\vec{p}||\vec{k}|}\left[|\vec{k}|Q_0(z) - |\vec{p}|Q_1(z)\right]\Psi_S(|\vec{p}|) = \int dr \frac{\Psi_S(r)}{r} \mathrm{e}^{-\mu r}(1+\mu r) j_1(kr), \tag{68}$$

$$\int \frac{p^2 dp}{2|\vec{p}||\vec{k}|}\left[|\vec{p}|Q_1(z) - |\vec{k}|Q_2(z)\right]\Psi_D(|\vec{p}|) = -\int dr \frac{\Psi_D(r)}{r} \mathrm{e}^{-\mu r}(1+\mu r) j_1(kr), \tag{69}$$

where $\Psi_S(r)$ and $\Psi_D(r)$ are the deuteron wave functions in the coordinate space.

Then the result for the function $\Psi_{P_{5,7}}$ with a BS kernel with pseudo-scalar one-boson exchange reads

$$\Psi_{P_{5,7}}(P_{lab}) = -g_\pi^2 \frac{2\sqrt{3}}{M_d E'_p} \int_0^\infty dr \, \frac{\mathrm{e}^{-\mu r}}{r}\,(1+\mu r)\,\mathrm{j}_1(rP_{lab})\,[N_u\,u(r) + N_w\,w(r)], \tag{70}$$

where $u(r)$ and $w(r)$ are the non-relativistic deuteron wave functions in the coordinate representation, and $g_\pi^2 \approx 14.5$ is the pion-nucleon coupling constant. The normalization factors are $N_u = \sqrt{2}$ (1) and N_w = -1 ($\sqrt{2}$) for Ψ_{P_5} (Ψ_{P_7}) waves.

With this definition of the negative-energy waves one may estimate the origin of the relativistic corrections computed within the non-relativistic limit as additional contribution to the impulse approximation diagrams, such as meson exchange currents and $N\bar{N}$ pair production currents. As an example we compute within the one-iteration approximation the amplitude $\mathcal{A}$ which turns out to have the simple form of a negative-energy wave contribution

$$\mathcal{A} = \mathcal{A}_0 \; + \; 32\sqrt{6}\pi P_{lab}^3 \left(\Psi_S - \frac{1}{\sqrt{2}}\Psi_D\right)\Psi_{P_5}. \tag{71}$$

Substituting (70) into the expression for the amplitude eq. (71), the relativistic corrections in the one-iteration approximation become

$$\begin{aligned}\delta\mathcal{A} &= -g_\pi^2 P_{lab}^3 \frac{192\sqrt{2}\pi}{M_d E'_p} \\ &\times \int_0^\infty dr\, \frac{\mathrm{e}^{-\mu r}}{r}\,(1+\mu r)\,\mathrm{j}_1(rP_{lab})\left[\sqrt{2}\,u(r) - w(r)\right]\left(\Psi_S - \frac{1}{\sqrt{2}}\Psi_D\right), \end{aligned} \tag{72}$$

which is similar to expressions obtained in non-relativistic evaluations of the so-called "catastrophic" and pair production diagrams in electro-disintegration processes of the deuteron [43] and which is also similar to results of computation of the triangle diagrams usually considered in the elastic pD processes [19, 20]. In our case these corrections may be represented as diagrams with meson exchange due to anti-nucleon degrees of freedom in the BS equation, as depicted in fig. 9. The remaining amplitudes $\mathcal{B}, \mathcal{C}, \mathcal{D}$ and, consequently, the cross section (54) and all the polarization observables (38) receive analogous corrections. From this it becomes clear that generic relativistic calculations, even in impulse approximation, contain already to some extent specific meson-exchange diagrams, i.e., pair production currents, and one should pay attention on the problem of double counting when computing relativistic corrections beyond the spectator mechanism.

9 Summary

In summary, we present an explicit analysis of various relativistic effects in elastic backward scattering of protons off deuterons within the Bethe-Salpeter formalism with a realistic interaction kernel. To have a well defined framework for our methodological investigations we rely here on the impulse approximation. This allows to identify and investigate separately the contributions of the positive-energy waves, Lorentz boost corrections and relativistic effects due to negative-energy waves. Particular attention is paid to the computation of the four spin amplitudes of the process within the Bethe-Salpeter approach. By writing these amplitudes in the center of mass system in a non-covariant form a direct correspondence between our approach and the general phenomenological analysis of the process is found. In such a way a suitable representation of the polarization observables and a straightforward investigation of the non-relativistic limit are achieved.

Numerical estimates of the Lorentz boost and other relativistic effects in the cross section and selected polarization observables, at kinematical conditions of ongoing and forthcoming experiments [1, 2] are presented. It is found that in a complete set of polarization observables, proposed for a reconstruction of the amplitude, relativistic corrections either

may be negligible for a certain class of spin-correlations or play a crucial role for other observables. It is shown that the one-nucleon exchange mechanism alone does not give the predominant contribution in these reactions and future experiments must clarify effects beyond the impulse approximation.

Acknowledgments

Useful discussions with A.Yu. Umnikov and F. Santos are gratefully acknowledged. Two of the authors (L.P.K. and S.S.S.) would like to thank for the warm hospitality of the nuclear theory group at the Research Center Rossendorf. This work has been supported in parts by a grant of the Heisenberg-Landau JINR-FRG collaboration project.

Appendix A

The covariant expression of the vertex function $\Gamma(D,q)$ for the BS equation with one particle on mass shell is rather known and may be found, for instance in refs. [17, 23, 33]. Here we present the covariant solution $\Gamma(D,q)$ for the full BS equation when both particles are off the mass shell

$$\Gamma(D,q) = [h_1\hat{\xi} + h_2\frac{(q\xi)}{m}] + \frac{\hat{D}/2+\hat{q}-m}{m}[h_3\hat{\xi} + h_4\frac{(q\xi)}{m}] +$$
$$[h_5\hat{\xi} + h_6\frac{(q\xi)}{m}]\frac{\hat{D}/2-\hat{q}+m}{m} + \frac{\hat{D}/2+\hat{q}-m}{m}[h_7\hat{\xi} + h_8\frac{(q\xi)}{m}]\frac{\hat{D}/2-\hat{q}+m}{m}. \qquad (A\,1)$$

The eight invariant scalars $h_i(Dq, q^2)$ are connected with the corresponding spin-orbit momentum vertex functions $g_i(p_0, P_{lab})$, which are numerically determined in the deuteron rest frame, via

$$\begin{aligned}
\sqrt{4\pi}h_1 \;=\; & \frac{\sqrt{2}}{16E_p^{'}M_d}(2E_p^{'} - 2p_0 + M_d)(M_d + 2p_0 + 2E_p^{'})g_1 + \\
& \frac{\sqrt{2}}{16E_p^{'}M_d}(-M_d + 2p_0 + 2E_p^{'})(2E_p^{'} - 2p_0 - M_d)g_2 - \\
& \frac{1}{16E_p^{'}M_d}(2E_p^{'} - 2p_0 + M_d)(M_d + 2p_0 + 2E_p^{'})g_3 - \\
& \frac{1}{16E_p^{'}M_d}(-M_d + 2p_0 + 2E_p^{'})(2E_p^{'} - 2p_0 - M_d)g_4 + \\
& + \frac{\sqrt{3}m}{16P_{lab}M_dE_p^{'}}(-M_d + 2p_0 + 2E_p^{'})(M_d + 2p_0 + 2E_p^{'})g_5 - \\
& \frac{\sqrt{3}m}{16P_{lab}M_dE_p^{'}}(2E_p^{'} - 2p_0 - M_d)(2E_p^{'} - 2p_0 + M_d)g_6, \qquad (A\,2)
\end{aligned}$$

$$
\begin{aligned}
\sqrt{4\pi}h_2 &= -\frac{\sqrt{2}m}{16(E_p^{'}+m)M_dE_p^{'}}(2E_p^{'}-2p_0+M_d)(M_d+2p_0+2E_p^{'})g_1- \\
&\frac{\sqrt{2}m}{16(E_p^{'}+m)M_dE_p^{'}}(-M_d+2p_0+2E_p^{'})(2E_p^{'}-2p_0-M_d)g_2- \\
&\frac{(m+2E_p^{'})m}{16(E_p^{'}-m)(E_p^{'}+m)E_p^{'}M_d}(2E_p^{'}-2p_0+M_d)(M_d+2p_0+2E_p^{'})g_3- \\
&\frac{(m+2E_p^{'})m}{16(E_p^{'}-m)(E_p^{'}+m)E_p^{'}M_d}(-M_d+2p_0+2E_p^{'})(2E_p^{'}-2p_0-M_d)g_4- \\
&\frac{\sqrt{3}m}{16pM_dE_p^{'}}(-M_d+2p_0+2E_p^{'})(M_d+2p_0+2E_p^{'})g_5+ \\
&\frac{\sqrt{3}m}{16pM_dE_p^{'}}(2E_p^{'}-2p_0-M_d)(2E_p^{'}-2p_0+M_d)g_6, \qquad \text{(A 3)} \\
\sqrt{4\pi}h_3 &= \frac{\sqrt{3}m}{8M_dP_{lab}}(-M_d+2p_0+2E_p^{'})g_5- \\
&\frac{\sqrt{3}m}{8M_dP_{lab}}(2E_p^{'}-2p_0+M_d)g_6, \qquad \text{(A 4)} \\
\sqrt{4\pi}h_4 &= \frac{\sqrt{2}m^2}{8(E_p^{'}+m)M_dE_p^{'}}(2E_p^{'}-2p_0+M_d)g_1+ \\
&\frac{\sqrt{2}m^2}{8(E_p^{'}+m)M_dE_p^{'}}(-M_d+2p_0+2E_p^{'})g_2- \\
&\frac{(E_p^{'}+2m)m^2}{8(E_p^{'}-m)(E_p^{'}+m)E_p^{'}M_d}(2E_p^{'}-2p_0+M_d)g_3- \\
&\frac{(E_p^{'}+2m)m^2}{8(E_p^{'}-m)(E_p^{'}+m)E_p^{'}M_d}(-M_d+2p_0+2E_p^{'})g_4+ \\
&\frac{\sqrt{3}\sqrt{2}m^2}{8M_dP_{lab}E_p^{'}}(-M_d+2p_0+2E_p^{'})g_7- \\
&\frac{\sqrt{3}\sqrt{2}m^2}{8M_dP_{lab}E_p^{'}}(2E_p^{'}-2p_0+M_d)g_8, \qquad \text{(A 5)} \\
\sqrt{4\pi}h_5 &= -\frac{m\sqrt{3}}{8M_dP_{lab}}(M_d+2p_0+2E_p^{'})g_5+ \\
&\frac{m\sqrt{3}}{8M_dP_{lab}}(2E_p^{'}-2p_0-M_d)g_6, \qquad \text{(A 6)} \\
\sqrt{4\pi}h_6 &= -\frac{m^2\sqrt{2}}{8(E_p^{'}+m)M_dE_p^{'}}(M_d+2p_0+2E_p^{'})g_1- \\
&\frac{m^2\sqrt{2}}{8(E_p^{'}+m)M_dE_p^{'}}(2E_p^{'}-2p_0-M_d)g_2+ \\
&\frac{(E_p^{'}+2m)m^2}{8(E_p^{'}-m)(E_p^{'}+m)E_p^{'}M_d}(M_d+2p_0+2E_p^{'})g_3+ \\
&\frac{(E_p^{'}+2m)m^2}{8(E_p^{'}-m)(E_p^{'}+m)E_p^{'}M_d}(2E_p^{'}-2p_0-M_d)g_4+
\end{aligned}
$$

$$\frac{\sqrt{3}\sqrt{2}m^2}{8M_dP_{lab}E_p^{'}}(M_d+2p_0+2E_p^{'})g_7 -$$
$$\frac{\sqrt{3}\sqrt{2}m^2}{8M_dP_{lab}E_p^{'}}(2E_p^{'}-2p_0-M_d)g_8, \quad \text{(A 7)}$$

$$\sqrt{4\pi}h_7 = \frac{\sqrt{2}m^2}{4M_dE_p^{'}}g_1+\frac{\sqrt{2}m^2}{4M_dE_p^{'}}g_2-\frac{m^2}{4M_dE_p^{'}}g_3$$
$$-\frac{m^2}{4M_dE_p^{'}}g_4-\frac{m^3\sqrt{3}}{4M_dP_{lab}E_p^{'}}g_5+\frac{m^3\sqrt{3}}{4M_dP_{lab}E_p^{'}}g_6, \quad \text{(A 8)}$$

$$\sqrt{4\pi}h_8 = \frac{\sqrt{2}m^3}{4(E_p^{'}+m)M_dE_p^{'}}g_1+\frac{\sqrt{2}m^3}{4(E_p^{'}+m)M_dE_p^{'}}g_2+$$
$$\frac{m^3(m+2E_p^{'})}{4(E_p^{'}-m)(E_p^{'}+m)E_p^{'}M_d}g_3+\frac{m^3(m+2E_p^{'})}{4(E_p^{'}-m)(E_p^{'}+m)E_p^{'}M_d}g_4$$
$$-\frac{m^3\sqrt{3}}{4M_dP_{lab}E_p^{'}}g_5+\frac{m^3\sqrt{3}}{4M_dP_{lab}E_p^{'}}g_6, \quad \text{(A 9)}$$

where $p_0=(Dq)/M_d$ and $E_p^{'}=\sqrt{P_{lab}^2+m^2}$. The spin-orbit momentum vertex functions are defined within the ρ spin classification as $g_1=S^{++}$, $g_2=S^{--}$, $g_3=D^{++}$, $g_4=D^{--}$, $g_5={}^3P^{+-}$, $g_6={}^3P^{-+}$, $g_7={}^1P^{+-}$, $g_8={}^1P^{-+}$.

Eqs. (A 2) - (A 9) may be written in a more compact form, however the present expressions are more informative and easily understood by the reader.

10 Appendix B

In obtaining eqs. (28) - (33) the following relations are useful

$$p\xi^{\prime}=\frac{E-\epsilon}{M_d}(\boldsymbol{p}\boldsymbol{\xi}^{\prime}), \quad p^{\prime}\xi=-\frac{E-\epsilon}{M_d}(\boldsymbol{p}\boldsymbol{\xi}), \quad \text{(B 1)}$$

$$([\mathbf{a}\times\mathbf{b}])([\mathbf{c}\times\mathbf{d}])=(\mathbf{ac})(\mathbf{bd})-(\mathbf{ad})(\mathbf{bc}), \quad \text{(B 2)}$$

$$-i\boldsymbol{\sigma}(\boldsymbol{p}\times\boldsymbol{\xi})(\boldsymbol{p}\boldsymbol{\xi}^{\prime})+i\boldsymbol{\sigma}(\boldsymbol{p}\times\boldsymbol{\xi}^{\prime})(\boldsymbol{p}\boldsymbol{\xi})=i\boldsymbol{\sigma}(\boldsymbol{\xi}\times\boldsymbol{\xi}^{\prime})p^2-i(\boldsymbol{\sigma}\boldsymbol{p})(\boldsymbol{p},\boldsymbol{\xi}\times\boldsymbol{\xi}^{\prime}), \quad \text{(B 3)}$$

$$\boldsymbol{a}=\boldsymbol{\xi}+\boldsymbol{p}\frac{\boldsymbol{p}\boldsymbol{\xi}}{M_d(E+M_d)}, \quad \boldsymbol{a}^{\prime}=\boldsymbol{\xi}^{\prime}+\boldsymbol{p}\frac{\boldsymbol{p}\boldsymbol{\xi}^{\prime}}{M_d(E+M_d)}, \quad \text{(B 4)}$$

$$(\boldsymbol{\sigma}\boldsymbol{a})(\boldsymbol{\sigma}\boldsymbol{a}^{\prime})=(\boldsymbol{\xi}\boldsymbol{\xi}^{\prime})+i\boldsymbol{\sigma}(\boldsymbol{\xi}\times\boldsymbol{\xi}^{\prime})\frac{E}{M_d}+\frac{\boldsymbol{p}\boldsymbol{\xi}}{M_d}\frac{\boldsymbol{p}\boldsymbol{\xi}^{\prime}}{M_d}-i(\boldsymbol{\sigma}\boldsymbol{p})(\boldsymbol{p},\boldsymbol{\xi}\times\boldsymbol{\xi}^{\prime})\frac{1}{M_d(M_d+E)}. \quad \text{(B 5)}$$

References

[1] I.M. Sitnik et al., JINR Rapid Communication 2(70)-95, p. 19, "The measurement of spin correlations in the reaction D+p → p+D (Proposal)", Dubna (1995).

[2] V.I. Komarov et al., COSY proposal 20 "Exclusive deuteron break-up study with polarized protons and deuterons at COSY";
V.I. Komarov et al., KFA Annual Rep. Jülich (1995) 64;
A.K. Kacharava et al., JINR Communication E1-96-42, Dubna, 1996.

[3] S.E. Kuhn et al., "The Spin-dependent Structure Function G_{1n} and the Q^2 Dependence of the Gerasimov-Drell-Hearn Sum Rule for the Neutron", CEBAF Proposal No. 93-009;
J.P. Chen, S. Gilad, Zh. Li and C.S. Whichat, "Helicity Structure of Pion Photoproduction on Polarized Deuteron and GDH Sum Rule for the Neutron", CEBAF Proposal, 94-117.

[4] F. Rotz, H. Arenhövel and T. Wilbois, nucl-th/9707045;
H. Arenhövel, W. Leidemann and L. Tomusiak, Phys. Rev. **C 52** (1995) 1232; Phys. Rev. **C 46** (1992) 455.

[5] M.P. Rekalo, N.M. Piskunov and I.M. Sitnik, E2-97-190, Preprint JINR, Dubna, 1997; E4-96-328, Preprint JINR, Dubna, 1996; Russian J. Nucl. Phys. **57** (1994) 2089.

[6] V.G. Ableev et al., Nucl. Phys. **A 393** (1983) 491;
C.F. Perdrisat and V. Punjabi, Phys. Rev. **C 42** (1990) 1899;
B. Kühn, C.F. Perdrisat and E.A. Strokovsky, Phys. Lett. **B 312** (1994) 298;
A.P. Kobushkin, A.I. Syamtomov, C.F. Perdrisat and V. Punjabi, Phys. Rev. **C 50** (1994) 2627;
J. Erö et al., Phys. Rev. **C 50** (1994) 2687;
J. Arvieux et al., Nucl. Phys. **A 431** (1984) 6132.

[7] M.P. Rekalo and I.M. Sitnik, Phys. Lett. **B 356** (1995) 434;
L.S. Azhgirei et al., Phys. Lett. **B 361** (1995) 21.

[8] V. Punjabi et al., Phys. Lett. **B 350** (1995) 178.

[9] S.L. Belostotski et al., Phys. Rev. **C 56** (1997) 50.

[10] S. Vasan, Phys. Rev. **D 8** (1973) 4092.

[11] L. Frankfurt and M. Strikman, Phys. Lett. **B 76** (1978) 285.

[12] V. Karmanov, Yad. Fiz. **34** (1981) 1020.

[13] V.P. Ladygin and N.B. Ladygina, E2-96-322, Preprint JINR, Dubna, 1996;
V.P. Ladygin, E2-96-333, Preprint JINR, Dubna, 1996.

[14] L.S. Azhgirei et al., 14th Int. IUPAP Conf. on Few Body Problems in Physics (ICFBP 14), Williamsburg, VA, 26-31 May 1994; Few-Body (ICFBP 14) (1994), 423;

[15] L.S. Azhgiey et al., Phys. Lett. **B 391** (1997) 22.

[16] L.S. Kisslinger, in "Mesons in Nuclei", p. 261, edited by M. Rho and D. Wilkinson; North-Holland, Amsterdam, 1978.

[17] B.D. Keister and J.A. Tjon, Phys. Rev. **C 26** (1982) 578.

[18] B.D. Keister, Phys. Rev. **C 24** (1981) 2628.

[19] N.S. Craigie and C. Wilkin, Nucl. Phys. **B 14** (1969) 477;
V.M. Kolybasov and N.Ya. Smorodinskaya, Phys. Lett. **B 37** (1971) 272.

[20] A. Nakamura and L. Satta, Nucl. Phys. **A 445** (1985) 706.

[21] A.Yu. Umnikov, hep-ph/9605292.

[22] A.Yu. Umnikov, L.P. Kaptari, K.Yu. Kazakov and F.C. Khanna, Phys. Lett. **B 334** (1994) 163.

[23] R.G. Arnold, C.E. Carlson and F. Gross, Phys. Rev. **C 21** (1980)1426;
F. Gross, J.W. Van Orden and K. Holinde, Phys. Rev. **C 45** (1992) 2094.
F. Gross, Phys. Rev. **186** (1969) 1448.

[24] L.P. Kaptari, A.Yu. Umnikov, S.G. Bondarenko, K.Yu. Kazakov, F.C. Khanna and B. Kämpfer, Phys. Rev. **C 54** (1996) 986.

[25] V. Ghazikhanian et al., Phys. Rev. **C 43** (1991) 1532;
G. Alberi, M. Bleszyansky and T. Jaroszewicz, Ann. Phys. **142** (1982) 299.

[26] S.G. Bondarenko, M. Beyer, V.V. Burov and S.M. Dorkin, nucl-th/9606035.

[27] S. Mandelstam, Proc. Roy. Soc. (London) **A 233** (1955) 123.

[28] J.J. Kubis, Phys. Rev. **D 6** (1972) 547;
M.J. Zuilhof and J.A. Tjon, Phys. Rev. **C 22** (1980) 2369.

[29] L.P. Kaptari, B. Kämpfer, S.M. Dorkin and S.S. Semikh, Phys. Lett. **B 404** (1997) 8.

[30] A.Yu. Umnikov and F.C. Khanna, Phys. Rev. **C 49** (1994) 2311.

[31] J. Fleischer and J.A. Tjon, Nucl. Phys. **B 84** (1975) 375;
Yu.L. Dorodnych et al., Phys. Rev. **C 43** (1991) 2499.

[32] A.Yu. Umnikov, L.P. Kaptaria and F.C Khanna, hep-ph/9608459, Phys. Rev. **C 56** (1997) in print.

[33] G. Rupp and J.A. Tjon, Phys. Rev. **C 41** (1990) 472.

[34] V. Noble and H.J. Weber, Phy. Lett. **B 50** (1974) 233.

[35] R. Machleid, K. Holinde and Ch. Elster, Phys. Rep. **149** (1987) 1.

[36] P. Berthet et al., J. of Phys. **G 8** (1982) L111;
L. Dubal et al., Phys. Rev. **D 9** (1974) 597.

[37] L.P. Kaptari, A.Yu. Umnikov, F.C. Khanna and B. Kämpfer, Phys. Lett. **B 351** (1995) 400.

[38] L.L. Frankfurt and M.I. Strikman, Phys. Rep., **76** (1981) 215.

[39] S.J. Brodsky et al., Phys. Rev. **D8** (1973) 4574;
J.B. Kogut, D.E. Soper, Phys. Rev. **D1** (1970) 2901;
S. Weinberg Phys. Rev. **150** (1966) 1313.

[40] M. Lacombe, B. Loiseau, J.M. Richard, R. Vin Mau, J. Côé, P. Pirés and R. de Tourreil, Phys. Rev. **C 21** (1980) 861.

[41] E.L. Lommon, Ann. Phys. **125** (1980) 309;
T. Sato, M. Kobayashia and H. Ohtsubo, Prog. Theor. Phys. **68** (1982) 840;
M. Gari and H. Hyuga, Z. Phys. **A 277** (1976) 291;
V.V. Burov and V.N. Dostovalov, Z. Phys. **C 326** (1987) 245.

[42] B. Desplanques, V.A. Karmanov and J.F. Mathiot, Nucl. Phys. **A 589** (1995) 697.

[43] J.A. Lock and L.L. Foldy, Ann. Phys. **93** (1975) 276.

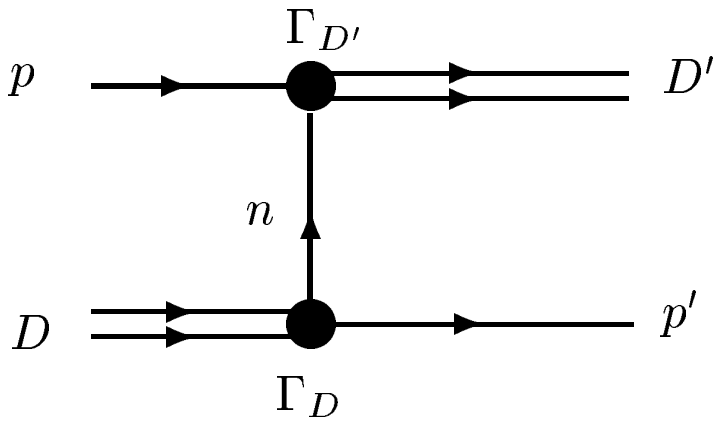

Figure 1: The one-nucleon exchange graph for the reaction $p + D = p'(\Theta = 180^o) + D'$.

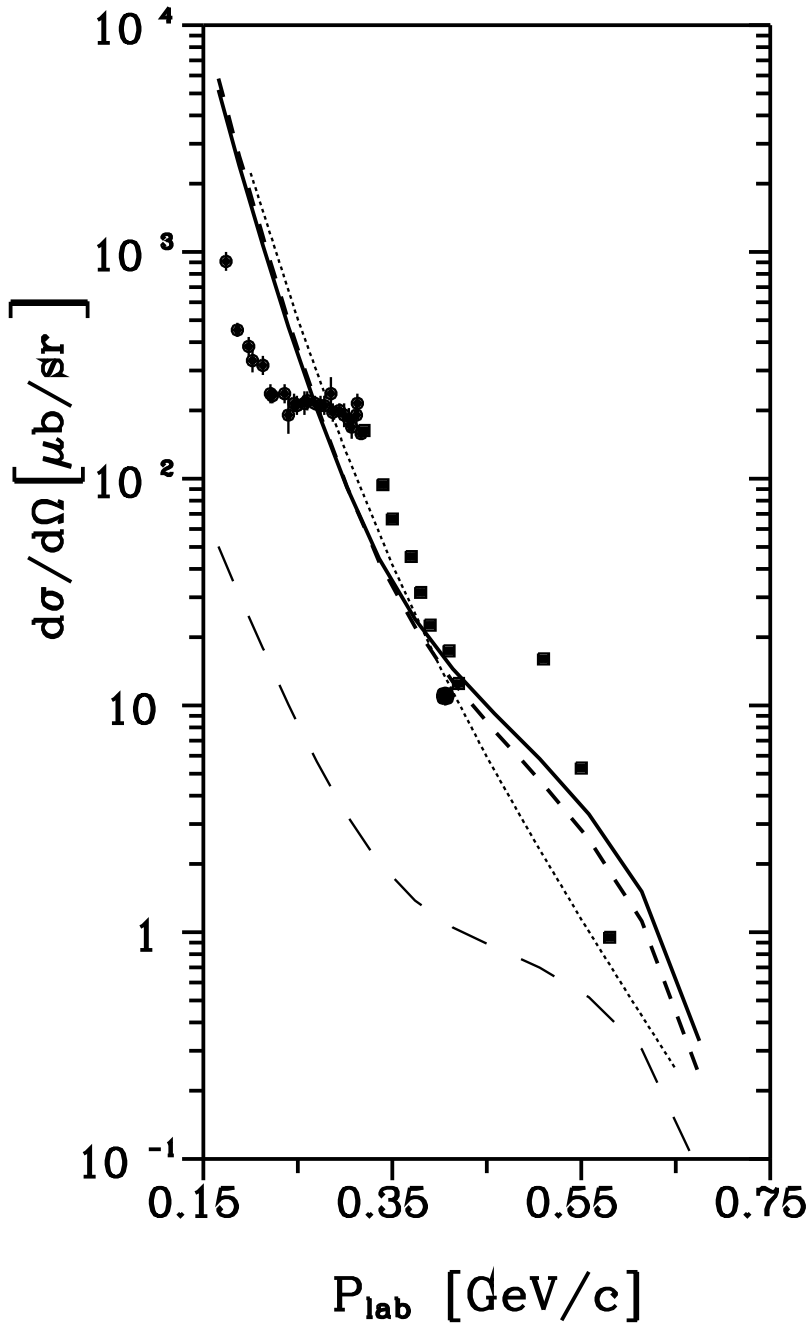

Figure 2: The spin averaged differential cross section $d\sigma/d\Omega$ for the elastic proton-deuteron backward scattering in the c.m.s. as a function of the momentum of the detected proton in the laboratory system. Dashed line: contribution of the positive-energy BS waves, long-dashed line: contribution of the Lorentz-boost effects eq. (51), solid line: full BS calculations, dotted line: results of calculations within the non-relativistic limit with the Bonn potential wave function. Experimental data from [20, 36].

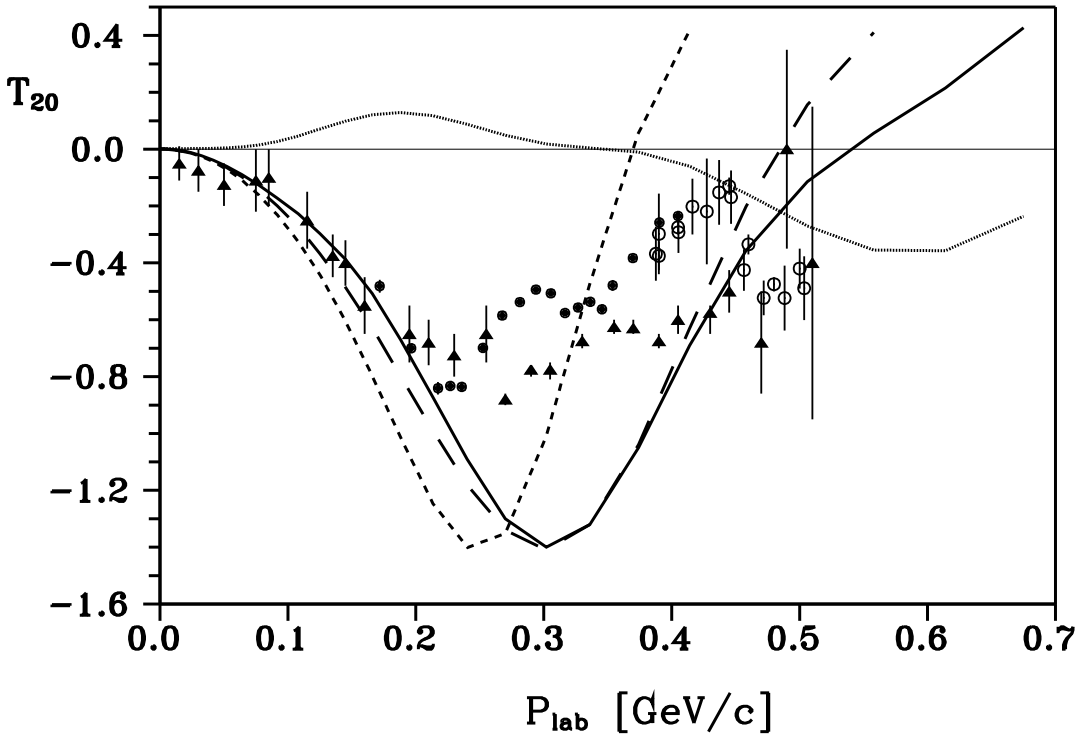

Figure 3: The deuteron tensor analyzing power T_{20} for the elastic proton-deuteron backward scattering. Long-dashed line: contribution of the positive energy BS waves eq. (52), dotted line: purely relativistic corrections computed by eq. (55), solid line: results of computation within the BS approach eq. (55), short-dashed line: results of computation within the minimal relativization scheme [39] with Paris potential wave function. Experimental data: circles - elastic backward scattering [7, 8, 14, 15], triangles - T_{20} measured in the deuteron break-up reaction [6].

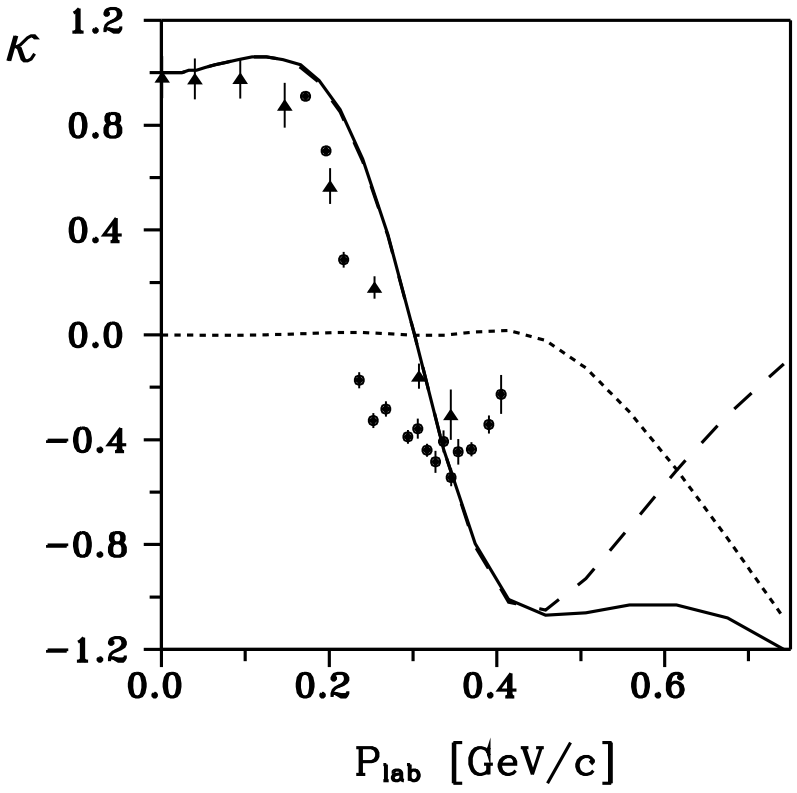

Figure 4: The polarization transfer κ for the elastic proton-deuteron backward scattering. Notation as in fig. 3.

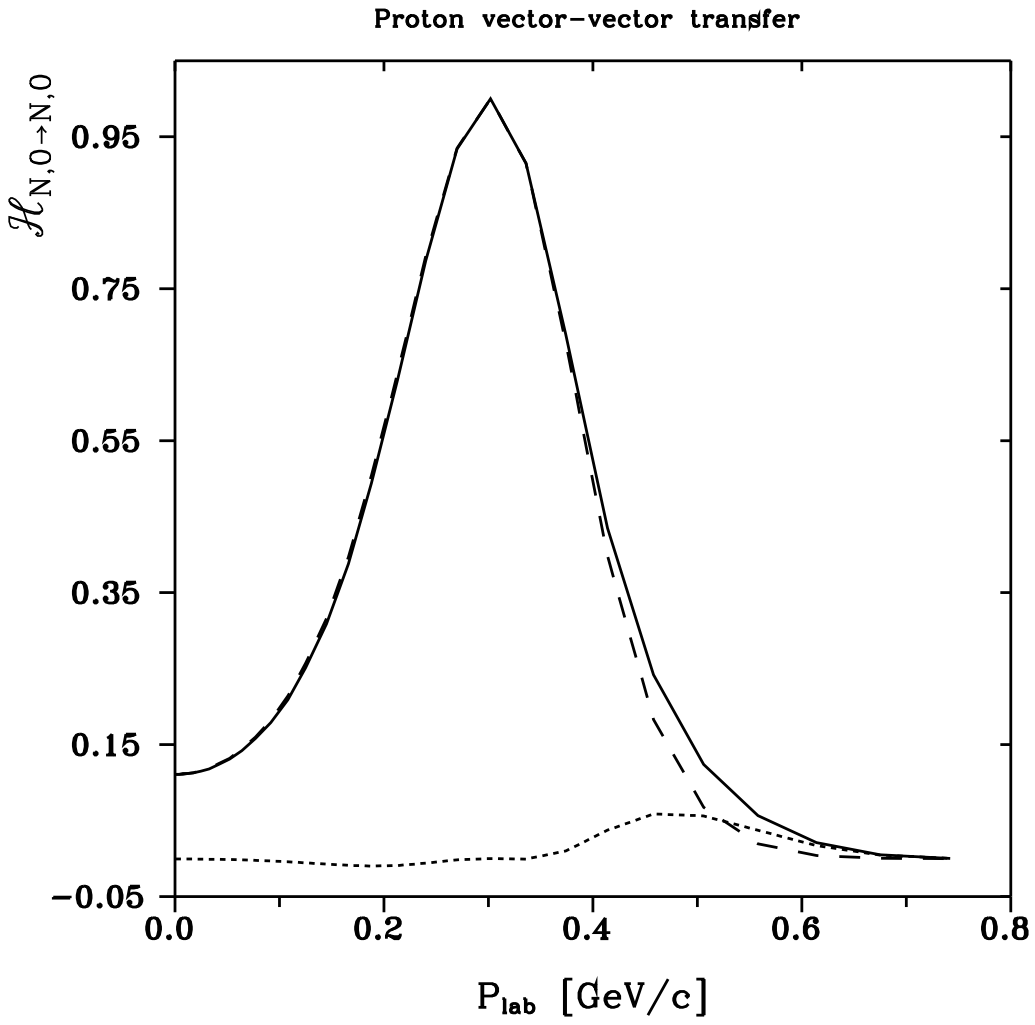

Figure 5: The vector-vector polarization transfer coefficient from the initial proton to the final proton. Dashed line: contribution of the positive-energy BS waves (i.e., the non-relativistic limit), dotted line: relativistic corrections, solid line: full BS results via eq. (57).

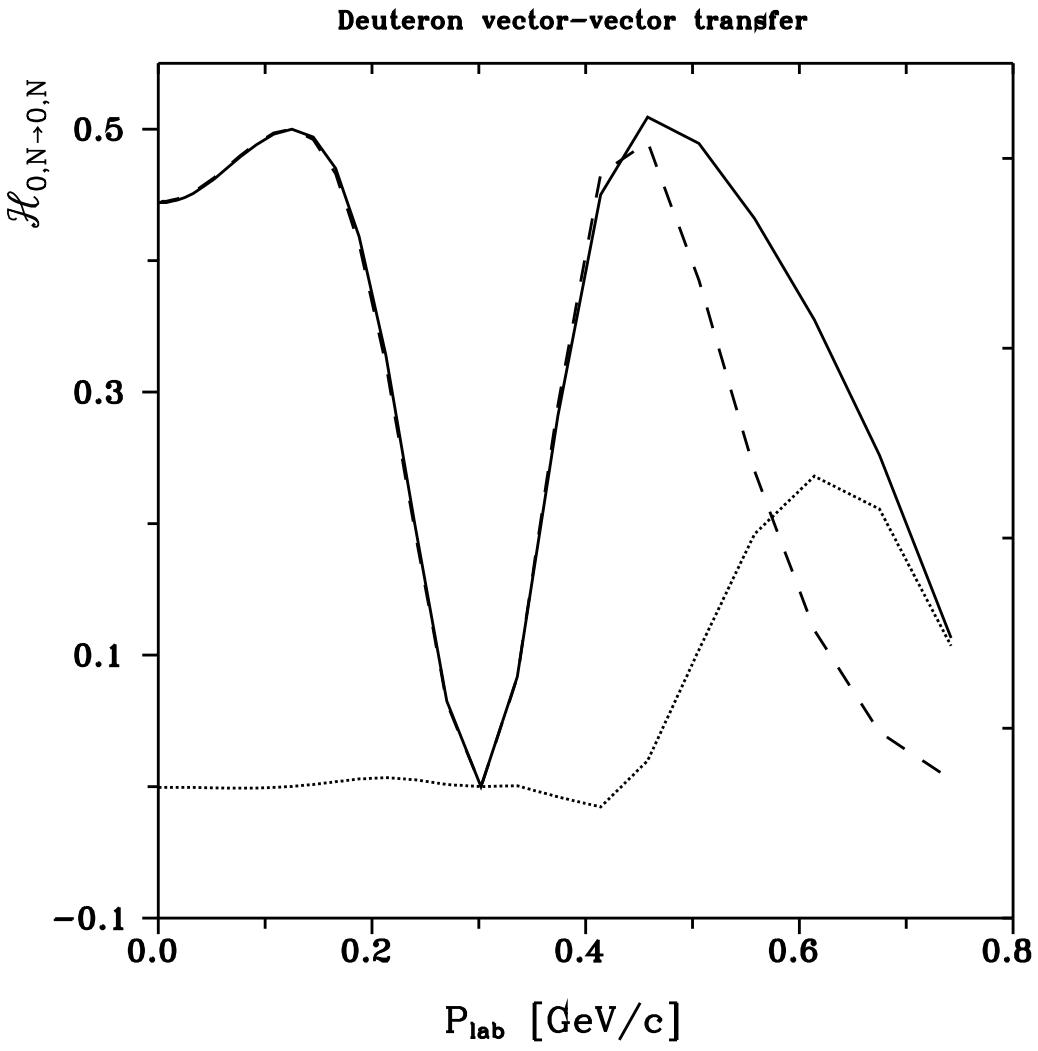

Figure 6: The vector-vector polarization transfer coefficient from the initial deuteron to the final deuteron. Notation as in fig. 5

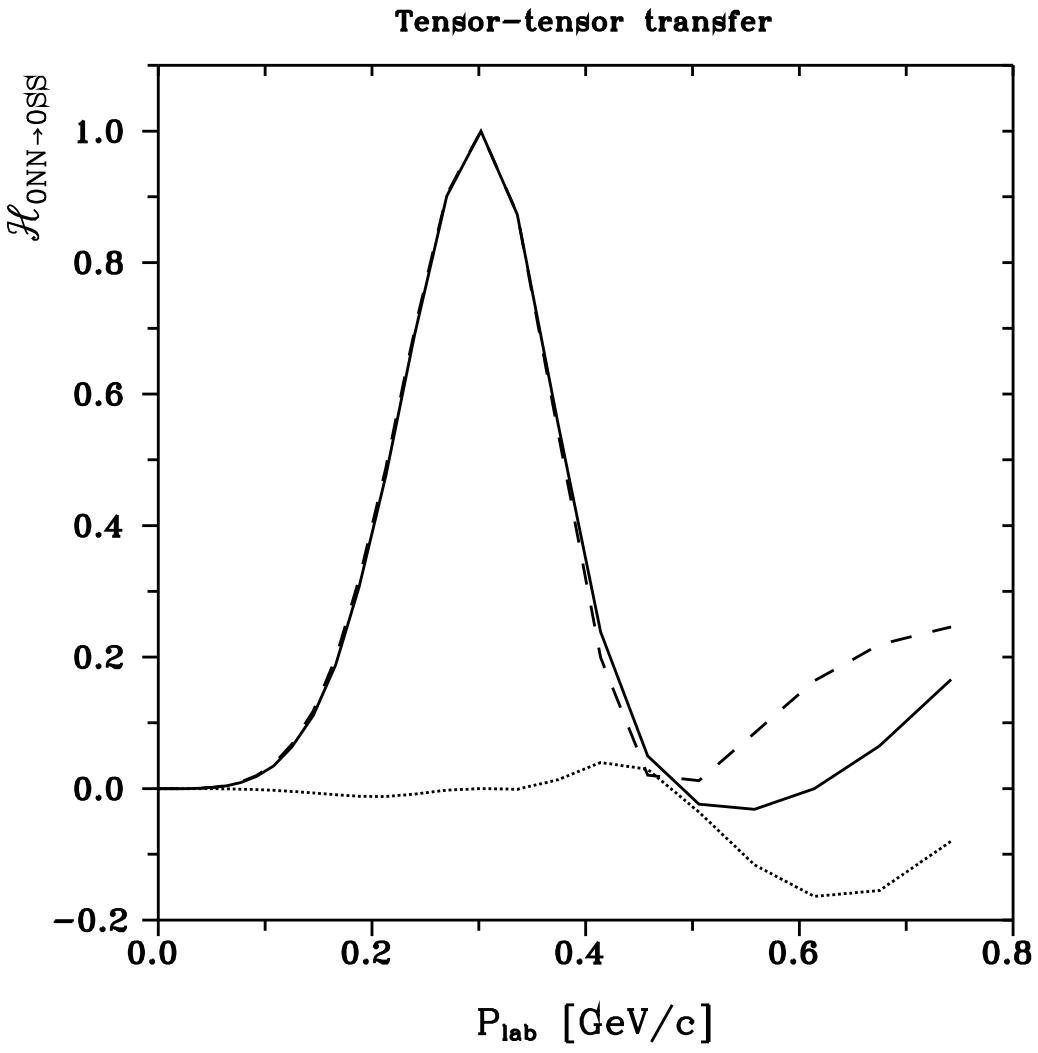

Figure 7: The tensor-tensor polarization transfer coefficient from the initial deuteron to the final deuteron. Notation as in fig. 5.

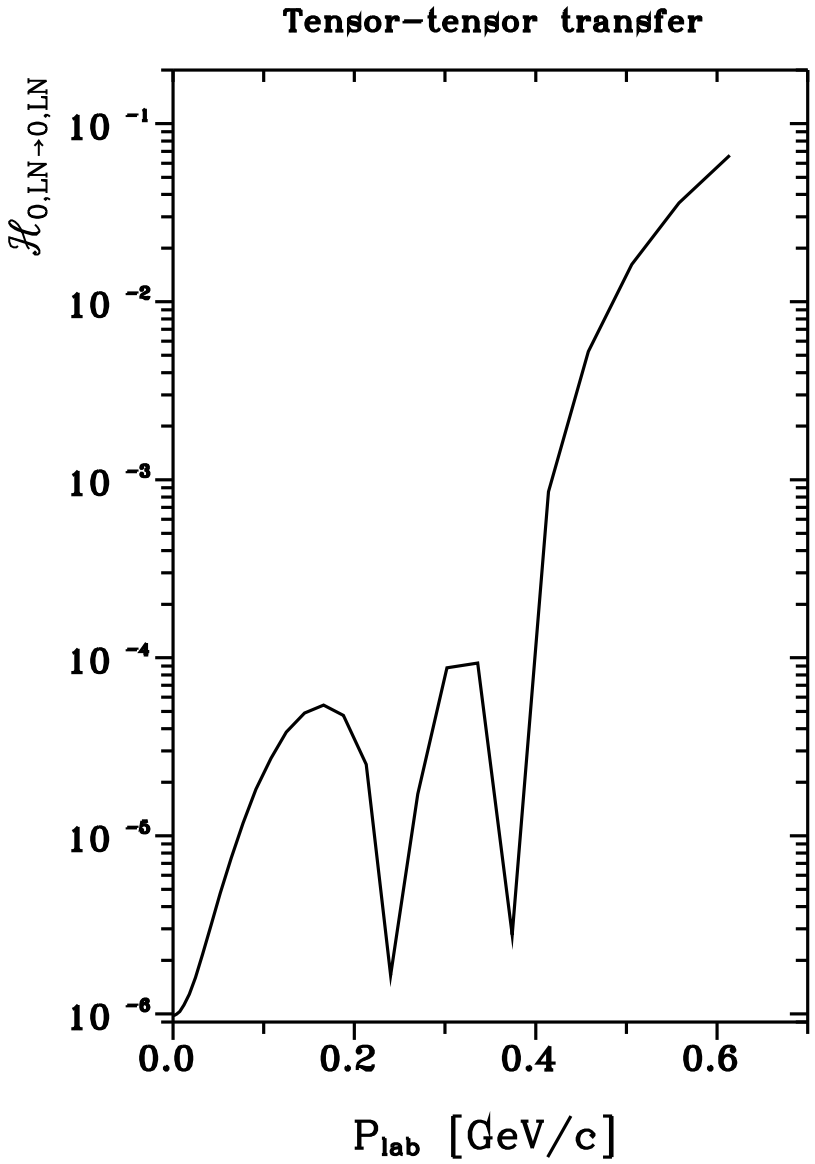

Figure 8: The relativistic corrections for the tensor-tensor polarization transfer coefficient from the initial deuteron to the final deuteron $\mathcal{H}_{0,LN\to 0,LN}$ defined by eq. (60). In the non-relativistic limit $\mathcal{H}_{0,LN\to 0,LN}$ vanishes.

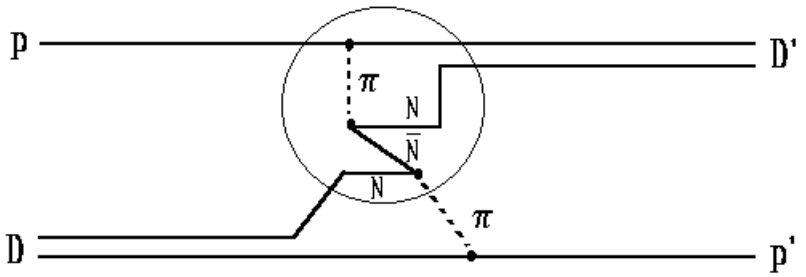

Figure 9: A possible intermediate mechanism already included in the one-nucleon exchange diagram in the BS approach.